

Investigation of an extreme rainfall event during 8–12 December 2018 over central Viet Nam – Part 2: An evaluation of predictability using a time-lagged cloud-resolving ensemble system

Chung-Chieh Wang¹, Duc Van Nguyen^{1,2}, Thang Van Vu², Pham Thi Thanh Nga², Pi-Yu Chuang¹, and Kien Ba Truong^{2,*}

Correspondence: kien.cbg@gmail.com

¹Department of Earth Sciences, National Taiwan Normal University, Taipei, Taiwan

²Viet Nam Institute of Meteorology, Hydrology and Climate Change, Hanoi, Viet Nam

Abstract:

This is the second part of a two-part study that investigates an extreme rainfall event that occurred from 8 to 12 December 2018 over central Viet Nam (referred to as the D18 event).

In this part, the study aims to evaluate the practical predictability of the D18 event using the quantitative precipitation forecasts (QPFs) from a time-lagged cloud-resolving ensemble ~~and a quantitative precipitation forecast~~ system. To do this ~~study~~, 29 time-lagged (8 days in ~~forecast range~~lead time) high resolution (2.5 km) members were run, with the first member initialized s-run at 12:00 UTC 3 December ~~2018~~, and the last one-member-run at 12:00 UTC 10 December 2018. Between the first and the last members are multiple members that were executed~~run~~ every 6-h. The evaluation~~ioned~~ results reveal that the cloud-resolving model (CReSS) well predicted the rainfall fields at the short-range ~~forecast~~ (less than 3 days) for 10 December (the rainiest day). Particularly, the results show CReSS show~~has~~ high skills in heavy-rainfall ~~quantitative precipitation forecasts (QPFs)~~ for this date~~24-h rainfall of 10 Dec~~ with the Similarity Skill Score (SSS)-~~scores~~ greater than 0.5 for both the last five members and the last nine members. ~~These~~ good results are due to the model having good predictions of relevant~~other~~ meteorological variables, such as surface wind ~~fields~~. However, ~~these~~ predictive~~on~~ skills is~~are~~ reduced~~ing~~ at ~~extending~~ lead times ~~(longer than 3 days)~~, and it is challenging to achieve ~~the prediction good of~~ QPFs for rainfall thresholds greater than 100 mm at~~with~~ lead times longer than 6 days. These

results also confirmed our scientific hypothesis that the cloud-resolving time-lagged ensemble system (using the CReSS model) improved the QPFs of this event at the short range. Furthermore, the results also demonstrated that a decent QPF can be made at a longer lead time (by a member initialized at 1800 UTC 4 December).

~~In addition~~Besides, the ensemble-based sensitivity analysis (ESA) of 24-hour rainfall in central Viet Nam ~~responds to the initial conditions~~ shows that ~~it~~~~the 24-hour rainfall~~ is ~~highly~~~~very~~ sensitive ~~to~~~~with~~ initial conditions, not only at ~~the~~ lower levels but also at ~~the~~ upper levels. The ~~rainfall is sensitive to both kinematics and moisture convergence at low levels, and such~~ensemble-based sensitivities ~~is~~ decreased with ~~the~~ increasing lead time. ~~Through the analysis of thermodynamic and moisture sensitivities, it showed that the features of the ensemble-based sensitivity analysis (ESA) also facilitates~~acilitated a better understanding of the ~~mechanisms in the D18 event, sensitivity of a precipitation forecast to the initial conditions~~, implying that it is meaningful to apply ESA to control initial conditions ~~by work~~ in the future.

1 Introduction

The present study is the second part of a two-part study investigating the extreme rainfall event during 8–12 December 2018 over central Viet Nam (referred to as the D18 event hereafter). ~~In this~~D18 event, ~~is a~~ record-breaking rainfall ~~event which~~ occurred along the mid-central coast ~~of Viet Nam~~, from Quang Binh to Quang Ngai provinces. The observational ~~data~~ shows that ~~the peak amount in rainfall accumulation, in particular, by heavy rainfall exceeded 800 mm over with the maximum a 3-days period accumulated rainfall from 12:00 UTC on 8 December to 12:00 UTC on 11 December exceeding 800 mm~~ (Fig. 1f). ~~During this period~~In ~~which~~, the rainiest day ~~was~~ 10 December with 24-h observed ~~amount~~~~data~~ exceeding 600 mm at some stations (Fig. 4 OBS). This record-breaking rainfall event led to 13 deaths, ~~widespread~~~~many~~ destructions in the environment ~~and~~, downstream cities, and ~~heavy~~~~many other~~ economic losses due to catastrophic flooding and landslides (Tuoi Tre news, 2018). In part 1 (Wang and Nguyen 2023), we focused on the analysis of the mechanism that caused this event and evaluated the simulation by the

Cloud-Resolving Storm Simulator (CReSS; Tsuboki and Sakakibara, 2002, 2007). The analysis results point out the main factors which led to this event as well as its spatial rainfall distribution. These factors included the combined interaction between the strong northeasterly winds and easterly winds over the South China Sea (SCS) in the lower troposphere (below 700 hPa). The local terrain also played essential role due to its barrier effect. The cloud model's good simulation results in part 1 indicated its promising potential in forecasting this event. Hence, in part 2, the present study focuses on an evaluation of its predictability of the D18 event through a series of time-lagged high-resolution ensemble quantitative precipitation forecasts (QPFs) by the CReSS model.

Until now, predicting heavy rainfall events is still challenging to meteorologists and weather forecasters, although great progresses have been made in the science of numerical weather prediction both computer science and atmospheric science have been made to improve predictability. The prediction of heavy to extreme rainfall is more difficult for Viet Nam, where both multi-scale interactions among different weather systems and strong influence by local topography often exist. For example, when D18 event occurred, several operational models were unable to predict this event successfully. Specifically, Fig. 1 shows the predictions for the D18 event by three global models at the National Centers for Environmental Prediction (NCEP), the European Centre for Medium-Range Weather Forecasts (ECMWF), and the Japan Meteorological Agency (JMA), and by one mesoscale regional model, the Weather Research and Forecasting (WRF) model, implemented for operation at the Mid-central regional Hydro-Meteorological center in Da Nang city, Viet Nam, with the finest horizontal grid spacing (Δx) of $6 \text{ km} \times 6 \text{ km}$. While these models overall made good predictions in the surface wind field, their 72-h accumulated rainfall amounts along the coast of central Viet Nam were (less than 250 mm and) were much lower than the observation, which exceeded 900 mm (Fig. 1). Therefore, in order to improve the QPFs for heavy rainfall events in Viet Nam, we need to not only understand their mechanisms of occurrence, but also adopt or develop better forecasting tools, more effective strategy, or both.

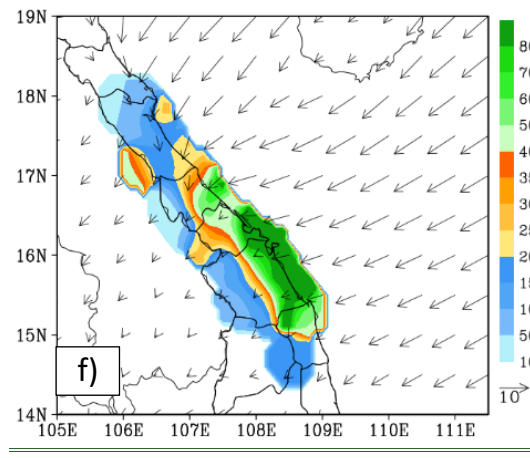
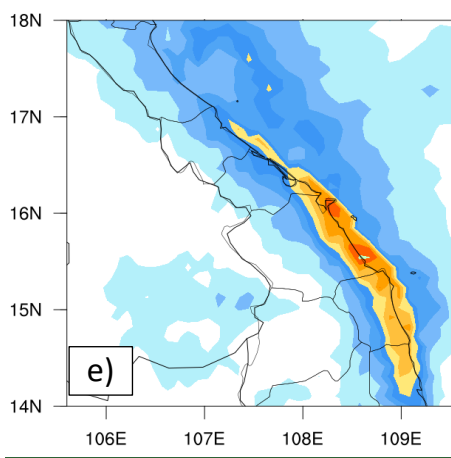
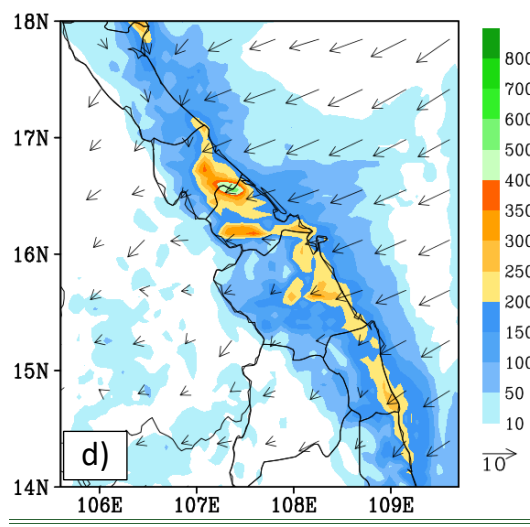
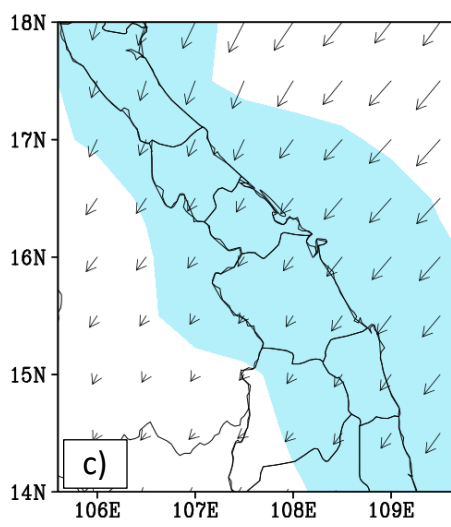
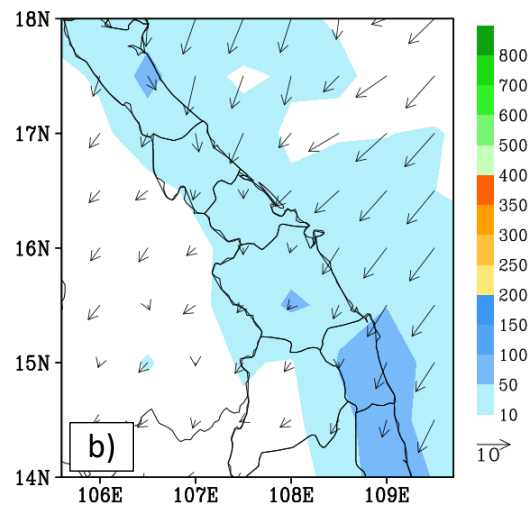
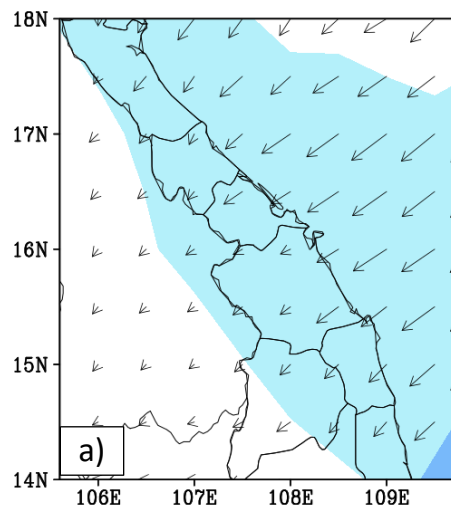
84

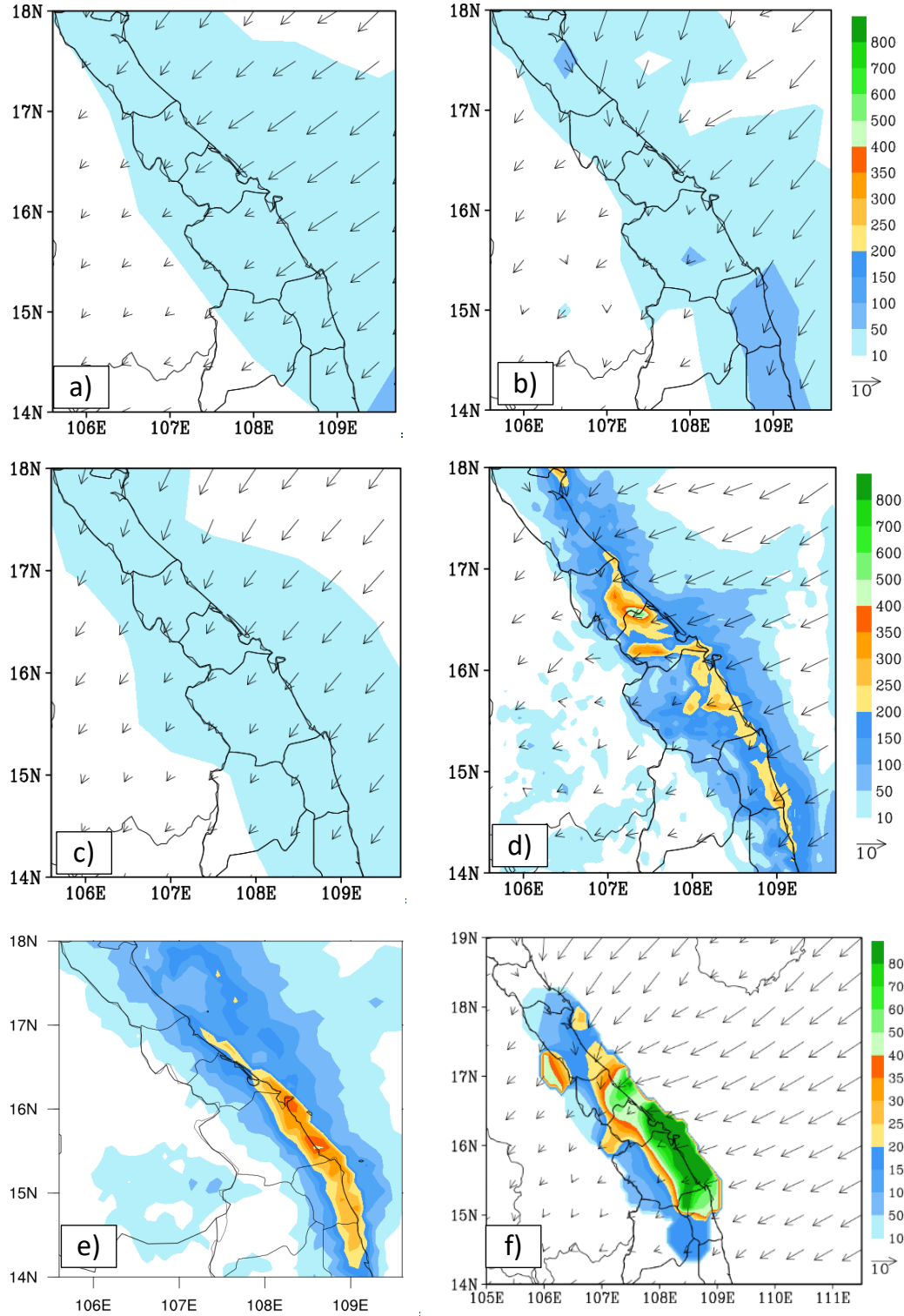
85

86

87

88





89

90 **Figure 1.** The predicted 72h accumulated rainfall (mm, shaded) and mean surface wind
 91 (ms^{-1} , vector) for the period of 12:00 UTC 8 December – 12:00 UTC 11 December 2018

obtained by (a) NCEP, (b) ECMWF, (c) JMA, (d) WRF, (e) 72h accumulated rainfall obtained by the Global Precipitation Measurement (GPM) estimate (IMERG Final Run product) and (f) 72h in-situ observed accumulated rainfall (mm, shaded) and the mean surface wind derived from ERA5 data (ms^{-1} , vector), adapted from Fig. 14c of Wang and Nguyen (2023).

Among several different methods, ~~the~~ present-day weather forecasts depend mainly on numerical weather prediction (NWP) using models, a scientific method that has become indispensable for its ability to simulate weather and produce quantitative results (Fig. 1).

However, there is always uncertainty in ~~the~~ numerical forecasts due to the fact that the atmosphere is a chaotic system and tiny errors in the initial state can grow rapidly and lead to larger errors in the forecast (Hohenegger and Schär, 2007, Lorenz 1969). Various approximations in numerical methods are also sources of forecast uncertainty. Thus, by generating a range of possible weather conditions in days ahead or into the future, the ensemble forecasting was introduced as an effective method to estimate forecast uncertainty and improve the overall accuracy and usefulness of NWP products. This is because ~~Furthermore, some studies show that the ensemble mean typically has smaller errors than individual members (Murphy 1988, Sureel et al. 2014). This error reduction is because since~~ the high predictability features that the members agree on are emphasized by the mean, while the low-predictability ones that the members do not agree on are filtered out or dampened (e.g., Leith 1974; Murphy 1988, Surcel et al. 2014).

~~Furthermore~~ For example, some studies have shown high skill in QPFs for extreme rainfall produced by typhoons in Taiwan using the CReSS model, a cloud-resolving model (CRM), with high resolution and time-lagged approach (Wang et al. 2016; Wang 2015; Wang et al. 2014; Wang et al. 2013). Table 1 of Wang et al. (2016) shows that the high-resolution time-lagged ensemble forecasts provide overall better quality in comparison with both the traditional low-resolution ensemble forecasts and high-resolution deterministic forecasts at a comparable cost in computation. ~~Furthermore, some studies show that the ensemble mean typically has smaller errors than individual members (Murphy 1988, Sureel et al. 2014).~~

~~This error reduction is because the high predictability features that the members agree on are emphasized by the mean, while the low predictability ones that the members do not agree on are filtered out or dampened (e.g., Leith 1974; Murphy 1988, Sorel et al. 2014).~~

Besides the advantages of ensemble forecasts described above, the ensemble-based sensitivity analysis (ESA) also ~~provides an~~^{helps} effective ~~method to~~^{ly} investigate how sensitive the forecast variables are and to what preceding factors. To be more specific, Torn and Hakim (2009) used ESA to evaluate how their subject, a group of tropical cyclones (TCs) undergoing extratropical transition, in the prediction respond to ~~a~~^{changes} in the initial condition. In their results, the cyclone minimum sea-level pressure forecasts are determined as strongly sensitive to TC intensity and position at short lead times and equally sensitive to mid-latitude troughs that interacted with the TC at longer lead times. For an extreme rainfall event in northern Taiwan, Wang et al. (2021) performed ESA using the results from 45 forecast members with ~~a~~^{grid sizes} of 2.5–5 km to identify contributing factors to heavy rainfall. By normalizing their impacts on rainfall using standard deviation (SD), different factors can be compared quantitatively and on an equal footing. Ranked by their importance, these factors included the position of the surface Mei-yu front and its moving speed, the position of 700-hPa wind shift line and its speed, the moisture amount in the environment near the front, timing and location of frontal mesoscale low-pressure disturbance, and frontal intensity. Many other studies also used the ESA to study TCs, convective events, or support the development of operational ensemble sensitivity-based techniques to improve probabilistic forecasts (e.g., Kerr et al. 2019, Hu and Wu 2020, Coleman and Ancell 2020).

While ensemble-based sensitivity analysis provides valuable insights into key drivers of forecast outcomes as reviewed above, its effectiveness is inherently tied to the limits of predictability. Generally, the atmospheric predictability can be categorized into two types: practical predictability and intrinsic predictability (Melhauser and Zhang 2012, Nielsen and Schumacher 2016, Ying and Zhang 2017, Weyn and Durran 2018). Intrinsic predictability represents the highest achievable predictability using a nearly perfect initial

conditions and a nearly perfect forecast model, and is mainly depended on scale and types of weather systems. Whereas, practical predictability describes the predictability using the best-available techniques and initial conditions, and therefore it can be limited by uncertainties in both the model and initial conditions. According to the studies cited above, practical predictability can be improved by improving the initial conditions, but it however cannot exceed the intrinsic predictability (Ying and Zhang 2017). Based on these, in our study, we investigate the practical predictability of the D18 event because it is a real event.

For heavy precipitation over central Viet Nam, Son and Tan (2009) used the Mesoscale Model version 5 (MM5) to investigate the predictability of heavy-rainfall events over the southern part of central Viet Nam during the period of 2005 and 2007. In this study, experiments were configured for two nested domains with Δx ~~the horizontal resolutions~~ of ~~the mother domain and the nest domain are~~ 27 km and 9 km, respectively. Their results showed that the MM5 can predict heavy rainfall there and its performance is better for events caused by TCs or TC interactions with the cold air. Toan et al. (2018) assessed the predictability of heavy rainfall events in middle-central Viet Nam due to combined effects of cold air and easterly winds using the WRF model within a forecast range of 2 days. The model was also set with two nesting domains. ~~The using the nesting technique. The~~ outermost domain (D1) covers the entirely Vietnam and SC ~~South China Sea~~ with a ~~Δx horizontal resolution~~ of 18 km, while the inner domain (D2) focuses on the Mid-Central Vietnam region with a ~~Δx horizontal resolutions~~ of 6 km. The evaluation indicated that ~~at for~~ 24-h lead time, the model performed reasonably well at rainfall thresholds less than 100 mm day⁻¹. ~~At the~~ ~~For~~ 48-h forecast range, the model performed well only at thresholds below 50 mm day⁻¹ and had some skill at 50–100 mm day⁻¹. However, heavy-rainfall events at thresholds over 100 mm day⁻¹ were almost unpredictable by the model. Nhu et al. (2017) also used the WRF model to investigate the role of the topography in central Viet Nam on the occurrence of a heavy-rainfall event there in November 1999. In this study, the model with triply3-nested domains with Δx horizontal resolution of 45 km, 15 km, and

5 km and 47 vertical levels well simulated the northeast monsoon circulation, TCs, and the occurrence of heavy rainfall in central Viet Nam. Furthermore, when the topography is removed, the three-day total accumulated rainfall decreased sharply (by approximately 75%) compared to that in the control experiment with the terrain. Hoa Van Vo (2016) examined the predictability of heavy-rainfall events during the wet seasons of 2008–2012 in the middle section and central highlands of Viet Nam using NWP products from several global models, including the Global Forecasting System (GFS) ~~offrom~~ NCEP, Global Spectral Model (GSM) ~~offrom~~ JMA, Navy Operational Global Atmospheric Processing System (NOGAPS) ~~offrom~~ the US Navy, and the Integrated Forecast System (IFS) ~~offrom~~ ECMWF. Their results indicated that the IFS and GSM performed better than the GFS and NOGAPS, and the IFS was evaluated the best. However, all four global models underestimated rainfall in extreme events. One of the reasons for this under-estimation~~ioned-rainfall~~ is that these models are global models, so their resolutions are too coarse ~~for~~while the relatively small study area ~~is too small~~.

The review above suggests that considerable limitations still exist in forecasting heavy rainfall in central Viet Nam, especially using coarser models. It also indicates that a high-resolution time-lagged ensemble approach may offer some advantages in the prediction of extreme rainfall events, such as a better simulation of local weather conditions, a quicker response to changes in forecast uncertainty in real time, and potentially a longer lead time for hazard preparation. Climatologically, the entire Viet Nam lies in the tropical zone (Fig. 2a), where vigorous but less organized convection often develops in response to local conditions. ~~This, while the~~ region is also prone to the influence and interactions of weather systems spanning a wide range of scales as reviewed. In addition, although central Viet Nam is a small region with the narrowest place only about 80 km in width, it possesses significant topography running in the north-south direction to affect rainfall (Fig. 2a). Hence, a high-resolution CRM with detailed and explicit treatment in cloud microphysics is likely crucial for better QPFs for heavy rainfall in central Viet Nam.

Given the above review and analysis, the scientific hypotheses are proposed: Storm-scale processes and convection were important in the D18 event. However, both global and mesoscale models with a grid size down to $6\text{ km} \times 6\text{ km}$ are not good enough for heavy-rainfall QPF without cloud-resolving capability (Fig. 1). Therefore, it is hypothesized that at higher resolution, the cloud-resolving time-lagged ensemble system (using the CReSS model) can improve the QPFs of this event at the short range. Additionally, this approach may also be able to extend the lead time of decent QPF beyond the short range. So, the goals of the study are to: 1) examine the hypothesis above, 2) investigate the (practical) predictability of this event through a series of time-lagged ensemble predictions, including whether a decent QPF can be made at a longer lead time, and 3) identify important factors leading to this event, including the lead time of the signals of these factors, using the ESA method. Consequently, the present study used the CReSS model to investigate the predictability of the D18 event through a series of time-lagged ensemble predictions. The rest of this paper is organized as follows. Section 2 describes the data, model, and methodology used in the study. The model results are presented and evaluated in Section 3. Finally, conclusions are offered in Section 4.

2 Data and methodology

2.1 Data

2.1.1 Model validation

2.1.1.1 In-situ observation data

The daily in-situ ~~observed~~ rainfall observations data (12:00–12:00 UTC, i.e., 19:00–19:00 LST) from 8 to 12 December 2018 at 69 automated gauge stations across central Viet Nam ~~are~~is used for case overview and verification of model results. This dataset is provided by the Mid-Central Regional Hydro Meteorological Center, Viet Nam. ~~The~~ spatial distribution of these gauge stations is depicted in ~~Ffig.ure~~Fig.ure 2b.

2.1.1.2 The Global Precipitation Measurement (IMERG Final Run V07) data

The Global Precipitation Measurement (GPM) is a joint international mission ~~international~~ ~~jointly-between~~ the National Aeronautics and Space Administration (NASA) and the Japan Aerospace Exploration Agency (JAXA), employing an ~~international~~ satellite network for advanced global rain and snow observations. The GPM *IMERG Final Run* is a research-level product which is created by intercalibrating, merging, and interpolating “all” satellite microwave precipitation estimates, along with microwave-calibrated infrared (IR) satellite estimates, analyses from precipitation gauges, and potentially other precipitation estimation methodologies at fine spatial and time ~~and-space~~ scales. The horizontal resolution of this dataset is $0.1^{\circ} \times 0.1^{\circ}$ latitude-longitude and the time ~~interval~~resolution is every 30 minute (Huffman et al. 2020). In this study, we used this satellite data (version 7) to verify rainfall distribution over the coastal sea due to the limitation of the ~~gaugeobservation-station~~ network, where we only have the observations exist only stations inland, as shown in ~~the~~ Fig. 2b. The GPM IMERGis dataset span was downloaded from 12:00 UTC ~~on 8-December~~ to 12:00 UTC ~~on 11 December 2018~~ and are used to analyze the D18 event as well as the rainiest day of this event (10 December).

2.1.1.3 The NCEP GDAS/FNL global tropospheric analyses data

The present study used this dataset (version d083003) to verify ~~the~~ initial data and ~~the~~ model outputs. The NCEP FNL analysis ~~data~~ is an operational global gridded analysis ~~data~~ and is freely provided by the NCEP. The horizontal resolution of this dataset is $0.25^{\circ} \times 0.25^{\circ}$ latitude-longitude with 26 levels extending from the surface to 10 hPa. The temporal ~~interval~~resolution is 6 hours. The vVariables ~~have been~~ used in this study including the zonal and meridional wind components, relative humidity, and vertical velocity at 925 hPa, covering the case period and downloaded from 18:00 UTC ~~04~~ to 12:00 UTC ~~09~~ December 2018.

2.1.2 The added values of CReSS ensemble

2.1.2.1 *The International Grand Global Ensemble retrieval*

In this study, we used the global model predictions to analyze the predictability of the D18 event. The International Grand Global Ensemble (TIGGE) retrieval is a key component of The Observing System Research and Predictability Experiment (THORPEX) research program, whose aim is to accelerate the improvements in the accuracy of 1-day to 2-week high-impact weather forecasts. The TIGGE retrieval provides not only deterministic forecast data but also ensemble prediction datasets from major centers, including NCEP of the USA, ECMWF of the European countries, and JMA of Japan, since 2006. This dataset has been used for a wide range of research studies on predictability and dynamical processes. The variables utilized included total precipitation and surface winds (~~u and v~~ ~~wind components~~ at 10-m height) from NCEP, ECMWF, and JMA at 6-h intervals during ~~the our~~ data period ~~(as shown in Figs. 1a-c)~~ from 12:00 UTC 8 to 12:00 UTC 11 December 2018 (as shown in Figs. 1a-c). ~~The data linked is placed in the “code and data availability” section.~~ The link to this dataset is placed in the “code and data availability” section.

2.2 The WRF data

~~The WRF is implemented for operational numerical forecast system at Mid-central regional Hydro-Meteorological center, Viet Nam. In this study, we used this data to analysis the predictability of D18 event using the mesoscale numerical prediction. The download variables include precipitation, the surface U wind component and surface V wind component. The lead time is 3 days, starting from 12:00 UTC 8 to 12:00 UTC 11 December 2018 with interval time of 6 hours. The horizontal resolution of this data is 6 km x 6 km.~~

2.2.1 Model description and experiment setup

We used the Cloud-resolving Storm Simulator model (CReSS). ~~This model had been built and~~ developed by Nagoya University, Japan (Tsuboki and Sakakibara, 2002, 2007). This is a non-hydrostatic and compressible cloud model, designed for simulation of various weather events at high (cloud-resolving) resolution. In the model, the cloud microphysics is treated explicitly at the user-selected degree of complexity, such as the bulk cold-rain scheme with six species: vapor, cloud water, cloud ice, rain, snow, and graupel (Lin et al.,

1983; Cotton et al., 1986; Murakami, 1990, 1994; Ikawa and Saito, 1991). Other subgrid-scale processes parameterized, such as turbulent mixing in the planetary boundary layer, ~~and as well as~~ physical options for surface processes, including momentum/energy fluxes, shortwave and longwave radiation, are summarized in Table 1.

~~For the initial and boundary conditions (IC/BCs)~~ Besides, the NCEP GFS ~~data (version ds084.6) from the~~ analyses and deterministic forecast runs, executed every 6 h, at 00:00, 06:00, 12:00, and 18:00 UTC daily (~~dataset ds084.6~~), were used to drive the CReSS model predictions. The horizontal resolution of the data is $0.25^\circ \times 0.25^\circ$, and 26 of vertical levels, and the forecast fields are provided every 3 h from the initial time out to a range of 192 h. The data ~~linked~~ is also placed in the “code and data availability” section.

To evaluate of the predictability of the D18 event using an ensemble time-lagged high-resolution system and investigate the ensemble sensitivity of variables for the rainfall, 29 experiments were performed. The first member was initialized ~~at~~ 12:00 UTC on 3 December ~~2018~~, and the last ~~one member was initialised~~ at 12:00 UTC on 10 December 2018. ~~Between them, a~~ A new member was initialized every 6 ~~h~~ and all members have a ~~within the period 1200 UTC 3 Dec 2018 1200 UTC 10 Dec 2018 (for a~~ simulation length of 192 h).

All experiments ~~using~~ a single domain at 2.5 km horizontal grid spacing and a dimension ~~in~~ (x, y, z) ~~dimension~~ of $912 \times 900 \times 60$ grid points (Table 1, cf. Fig. ~~ure~~ 2). As ~~mentioned~~ introduced above, the NCEP GFS was used as the IC/BCs of the CReSS model.

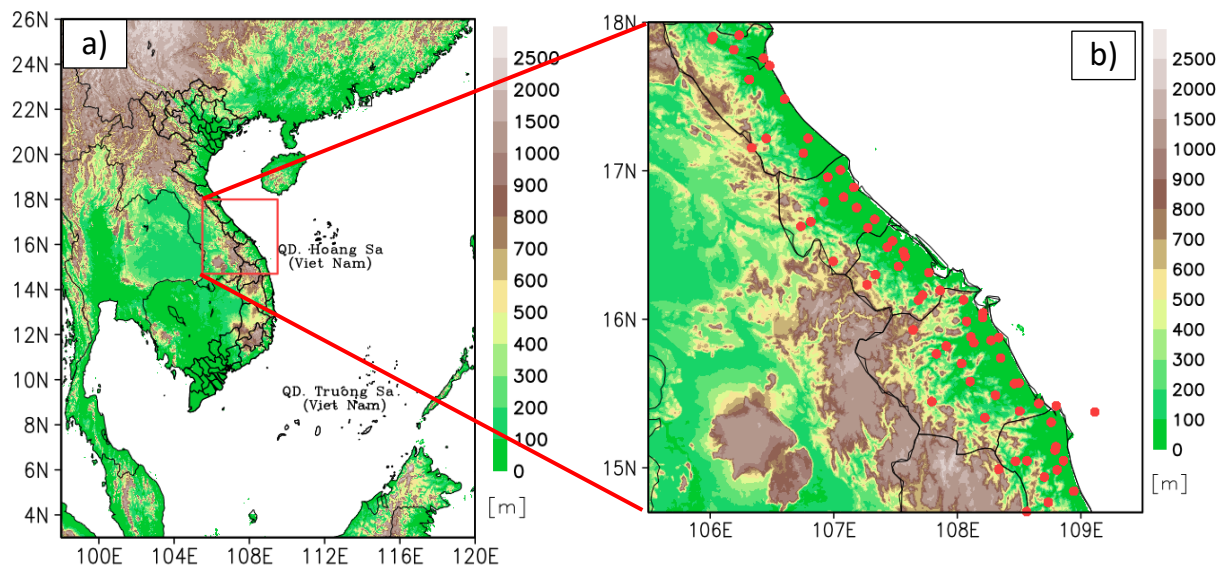


Figure 2. (a) The simulation domain of the CReSS model and topography (m, shaded) used in the study. (b) The distribution of the observation stations (red dots) in the study area.

Table 1. The basic information of experiments.

Domain and Basic setup	
Model domain	3°–26°N; 98°–120°E
Grid dimension (x, y, z)	912 × 900 × 60
Grid spacing (x, y, z)	2.5 km × 2.5 km × 0.5 km*
Projection	Mercator

IC/BCs (including SST)	NCEP GDAS/FNL Global Gridded Analyses and Forecasts ($0.25^\circ \times 0.25^\circ$, every 6 h, 26 pressure levels)
Topography (for CTRL only)	Digital elevation model by JMA at $(1/120)^\circ$ spatial resolution
Simulation length	192 h
Output frequency	1 hour
Model physical setup	
Cloud microphysics	<u>Double-moment</u> Bulk cold-rain scheme (six species, <u>Lin et al., 1983; Cotton et al., 1986; Murakami, 1990, 1994; Ikawa and Saito, 1991</u>)
PBL parameterization	1.5-order closure with prediction of turbulent kinetic energy (Deardorff, 1980; Tsuboki and Sakakibara, 2007)
Surface processes	Energy and momentum fluxes, shortwave and longwave radiation (Kondo, 1976; Louis et al., 1982; Segami et al., 1989)
Soil model	41 levels, every 5 cm deep to 2 m

* The vertical grid spacing (Δz) of CReSS is stretched (smallest at bottom) and the averaged value is given in the parentheses

2.3 Verification of model rainfall

In order to verify ~~the~~ model ~~simulated~~ ~~simulated~~ rainfall, some verification methods are used, including (1) visual comparison between the model and the observation (from the 69 automated gauges over the study area), and (2) ~~the~~ objective verification using categorical

skill scores at various rainfall thresholds from the lowest at 0.05 mm up to 900 mm for three-day total. These scores are presented below along with their formulas and interpretation, perfect value, and worst value, respectively. To apply these scores at a given threshold, the model and observed value pairs at all verification points N (gauge sites here, ~~N~~) are first compared and classified to construct a 2×2 contingency table (Wilks, 2006). At any given site, if the event takes place (reaching the threshold) in both model and observation, the prediction is considered a hit (H). If the event occurs only in observation but not the model, it is a miss (M). If the event is predicted in the model but not observed, it is a false alarm (FA). Finally, if both model and observation show no event, the outcome is correct rejection (CR). After all the points are classified into the above four categories, the categorical scores can be calculated by their corresponding formula as:

$$\text{Bias Score (BS)} = (H + FA) / (H + M), \quad (1)$$

$$\text{Probability of Detection (POD)} = H / (H + M), \quad (2)$$

$$\text{False Alarms Ratio (FAR)} = FA / (H + FA), \quad (3)$$

$$\text{Threat Score (TS)} = H / (H + M + FA), \quad (4)$$

The values of TS, POD, and FAR are all ranged from 0 to 1, and the higher ~~value is~~ the better for both TS and POD, but the opposite and conversely for FAR. For BS, its possible value can vary from 0 to $N=1$ and indicate ~~the~~ overestimation (underestimation) by of the model for the events if greater than (less than) unity.

2.3.1 The Similarity Skill Score

In addition to the categorical scores, the Similarity Skill Score (SSS, Wang et al., 2022) is also applied to evaluate the model rainfall results, as

$$SSS = 1 - \frac{\frac{1}{N} \sum_{i=1}^N (F_i - O_i)^2}{\frac{1}{N} \sum_{i=1}^N F_i^2 + \frac{1}{N} \sum_{i=1}^N O_i^2} \quad (5)$$

where N is the total number of verification points as before, and F_i is the forecast rainfall amount, and O_i is the observed ~~valuevalue~~, at the i th point among N , respectively. The SSS is a measure against the worst mean squared error (MSE) possible. The formula shows that a forecast with perfect skill has an SSS of 1, while a score of 0 means zero skill ~~(when the~~ model rainfall does not overlap with the observation anywhere).

2.3.2. The ensemble spread (standard deviation)

The ensemble spread is ~~considered~~ a measure of the difference ~~amongbetween~~ the members ~~about~~ to the ensemble mean, and ~~one suitable parameter is known as~~ the standard deviation (SD). In other words, the ensemble spread ~~will~~ reflects the diversity of all possible outcomes. Hence, the ensemble spread is often applied to ~~describepredict~~ the magnitude of the forecast errors. For example, a small spread indicates high theoretical forecast accuracy (and low uncertainty), and vice versa for a large spread ~~indicates low theoretical forecast accuracy~~. Using the SD, the sSpread is computed by the formulated below:

$$SD = \sqrt{\frac{\sum_{i=1}^n (x_i - \mu_x)^2}{n-1}} \quad (6)$$

where x_i is the ~~prediction~~ value of member i , for the variable x , μ_x is the ensemble mean, and n is the total number of ensemble members, respectively.

2.3.3. Ensemble Sensitivity Analysis

As mentioned above, an ensemble forecast is a set of forecasts produced by many separate forecasts typically with ~~different~~ ~~tees in~~ initial conditions, ~~respectively~~. Moreover, as we know, ~~NWP outcomes~~ ~~the numerical weather forecasts~~ are often sensitive to small changes in ~~ICinitial conditions~~ and the sensitivity analysis is considered a ~~methodmeasure~~ to improve forecasts through targeting observations. Hence, this study used the ESA method ~~which is~~ introduced by Ancell and Hakim (2007) to examine how a forecast variable

responds to changes in ICinitial-conditions. The ensemble sensitivity is computed by the formula:

$$\frac{\partial R}{\partial x_t} = \frac{COV(R, x_t)}{VARvar(x_t)} \quad (7)$$

Here, the response function R is chosen to be the areal-mean 24-h accumulated rainfall in central Viet Nam (15.5°-16.3°N, 107.9°-108.6°E) on the rainiest day, from 12:00 UTC on 9 to 12:00 UTC on 10 December 2018. The starting time of this period, i.e., 12:00 UTC on 9 December, is defined as t_0 . Various scalar variables are considered for x_t , while at a time ~~these~~ from 48 h earlier (t_{-48} , or 12:00 UTC on 7 December) to ~~the time of~~ t_0 at 24-h intervals. The COV is the covariance of R and x_t , and ~~VAR~~ var is the variance of x_t , respectively.

~~Since~~As the analysis in part 1 has identified that, the D18 event ~~was~~ caused by the combined ~~effectively~~ between the atmospheric disturbances at lower levels, such as the cold surge ~~and~~, easterly wind, and the topography, ~~the ensemble-based sensitivity analysis (ESA) herein~~ has been applied ~~to~~ for selected variables at surface, near-surface, and mid-tropospheric levels to assess the sensitivity of the rainfall field to ICinitial-conditions ~~and to its~~ the predictability ~~of the rainy field~~. In order to facilitate the comparison among the impacts of different variables, this study normalized ESA results by using the standardized anomaly in the denominator of Eq. (7) and expressed them as the change in R (in mm) in response to an increase in x_t by one SD in subsequent sections.

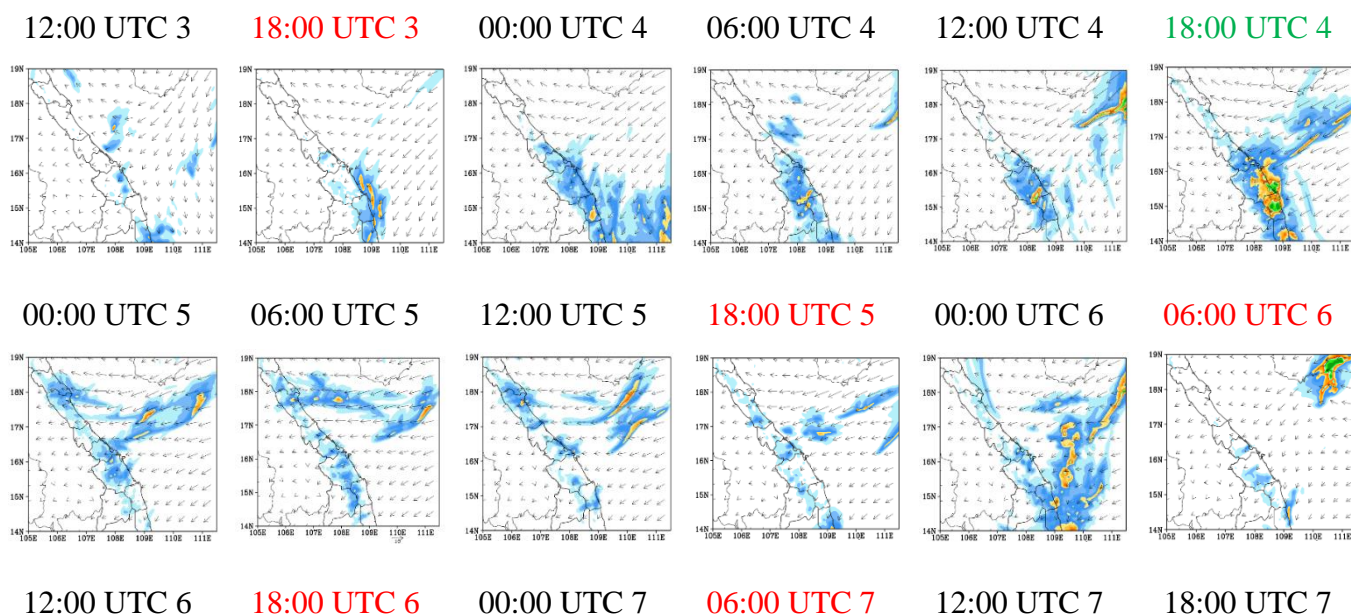
3 Model results

3.1 Time-lagged 24-h QPFs by the CReSS model

In this section, time-lagged forecasts targeted for the 24-h period from 12:00 UTC on 9 to 12:00 UTC on 10 December in the D18 event by the 2.5-km CReSS model are presented and evaluated. ~~This study focuses on this~~ 24-h period is chosen because ~~it~~ this is the rainiest day ~~with with 24-h~~ in-situ observationed ~~data~~ exceeding 600 mm at some stations (Fig. 3 OBS). Figure 3 shows 25 possible scenarios of 24-h rainfall and average surface winds

390 over the target period produced by the lagged runs every 6 h, with the earliest initial time
 391 at 12:00 UTC ~~on~~ 3 December and the latest one at 12:00 UTC ~~on~~ 9 December 2018;
 392 respectively. This is true for a well calibrated ensemble, only. It is immediately clear that
 393 several members made a rather good 24-h QPF not only in amounts, but also in rainfall
 394 location and spatial distribution. These include most members ~~starting~~initialised during 8-
 395 9 December, and also an impressive member ~~from that initialised at~~ 18:00 UTC ~~on~~ 4
 396 December. In this latter run-member, a reasonably good QPF was produced at a rather long
 397 lead time, almost five days (114 h) prior to the beginning of the target period (~~114 h~~). A
 398 common feature among these good members is that they all captured the direction and
 399 magnitude of surface winds quite well. On the other hand, most other members were less
 400 ideal~~did poorly~~ in their QPFs, when initialized before 06:00 UTC on 7 December at lead
 401 times beyond two days (before the target period). In general, they also dide~~could~~ not predict
 402 the surface winds well enough.

403



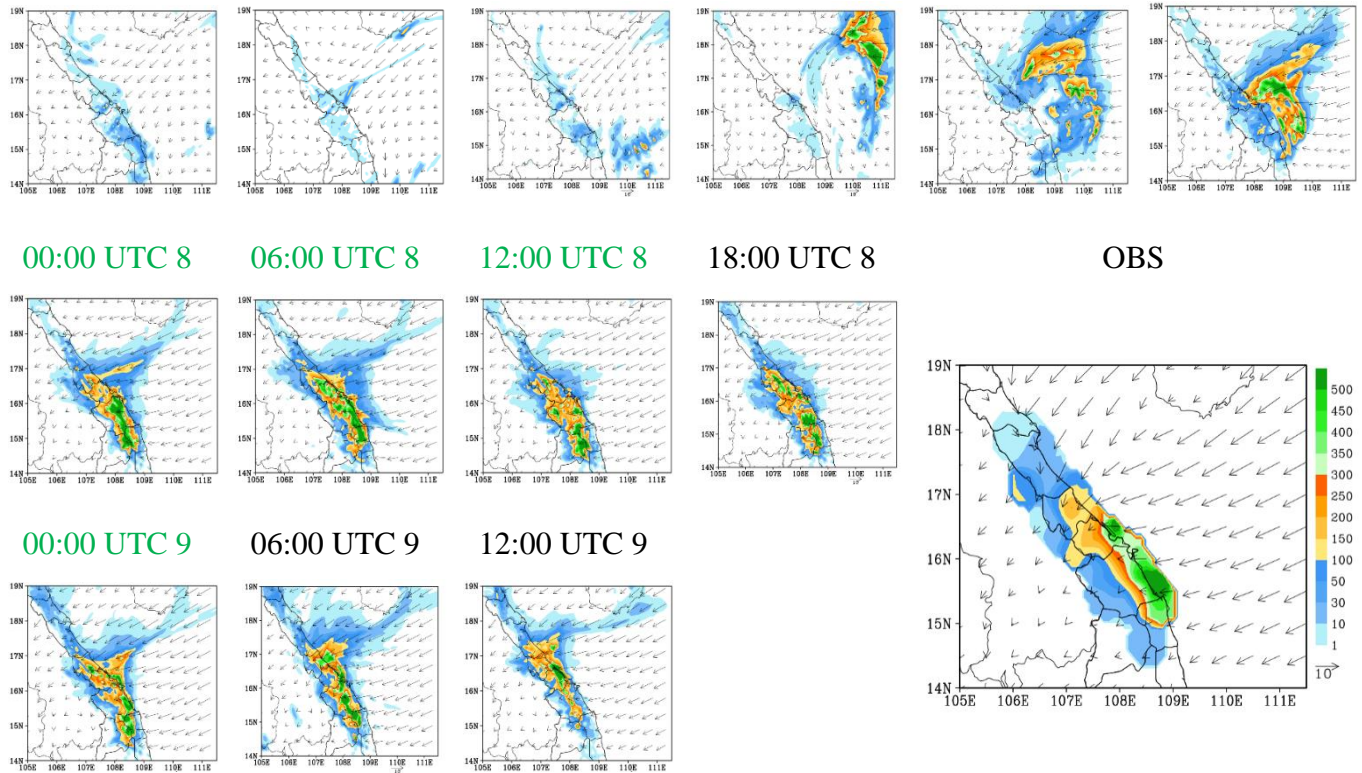
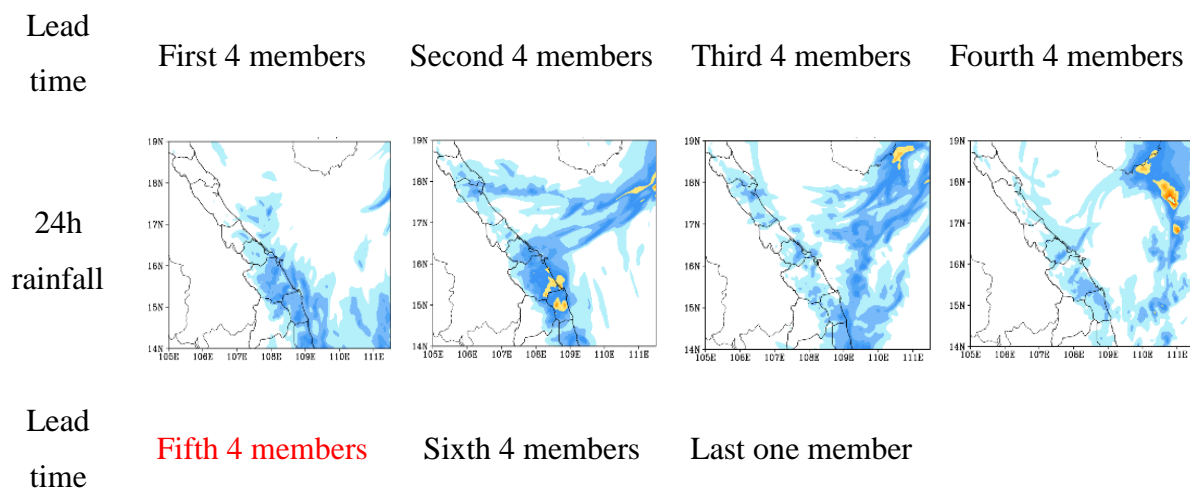


Figure 3. The predicted 24h accumulated rainfall (mm, shaded, scale on the right of panel OBS) and the mean surface horizontal wind (ms^{-1} , vector, reference length at panel OBS) on 10 December 2018 (from 12:00 UTC 9 December to 12:00 UTC 10 December 2018). The green color mark good members and the red color marks bad members. In OBS, 24h in-situ observed rainfall (mm, shaded) and the surface wind derived from ERA5 data (ms^{-1} , vector), adapted from Fig. 12f of Wang and Nguyen (2023).

Furthermore, as we know, ensemble weather forecasts are a set of forecasts from multiple members that represent the range of future weather possibilities, and the simplest way to use them is through the ensemble mean, which ~~(that~~ emphasizes the features that the members agree upon~~)~~. In order to see how well the 2.5-km good CReSS can predict the D18 event with the time-lagged strategy in terms possible scenarios of 24-h accumulated rainfall for, from possible scenarios of 24-hours of rainfall of 10th December that produced by CReSS, lagged runs are This study has grouped based on scenarios and computed them into different lead times using their range of ~~their~~ initial times in Fig. 4. It can be clearly seen in Fig. 4 that the rainfall predictions produced by the fifth Fifth four4- (executed between

12:00 UTC 7 ~~and~~ 06:00 UTC 8 December) and the ~~s~~ixth ~~four~~4 members (between 12:00 UTC 8 ~~and~~ 06:00 UTC 9 December) ~~members are~~ quite similar to ~~the~~ observed data, not only ~~in~~ rainfall amount but also ~~in~~ the locations of ~~significant rainbands and regions that concentratede mainly~~ rainfall. For other subgroup ~~scenarios~~, the model made the rainfall ~~wasseenarios~~ much lower than ~~the~~ observed rainfall in their scenarios data. In which, ~~the rainfall accumulations from the~~ third 4 (12:00 UTC 5 ~~to~~ 06:00 UTC 6 December) and fourth ~~four~~4 (12:00 UTC 6 ~~to~~ 06:00 UTC 7 December) members are the lowest. ~~OneIt can be~~ relevant ~~assessment~~ to the ~~outcome of these eight runs ismodel~~ that ~~none of them did not~~ predicted ~~well~~ the surface wind field ~~well enoughs at their in every single running at extend ranges (beyond threeafter days3), as discussedanalyzed previously.~~ On the other hand, ~~t~~he mean rainfall ~~efrom the~~ second ~~four members~~4 (12:00 UTC 4 ~~to~~ 06:00 UTC 5 December) ~~members~~ is the ~~best amonge highest allin these subgroups at the extended rangesenarios~~ due to a single good forecast initialized at 18:00 UTC on 4 December [cf. Fig. 3- (18:00 UTC 4)].



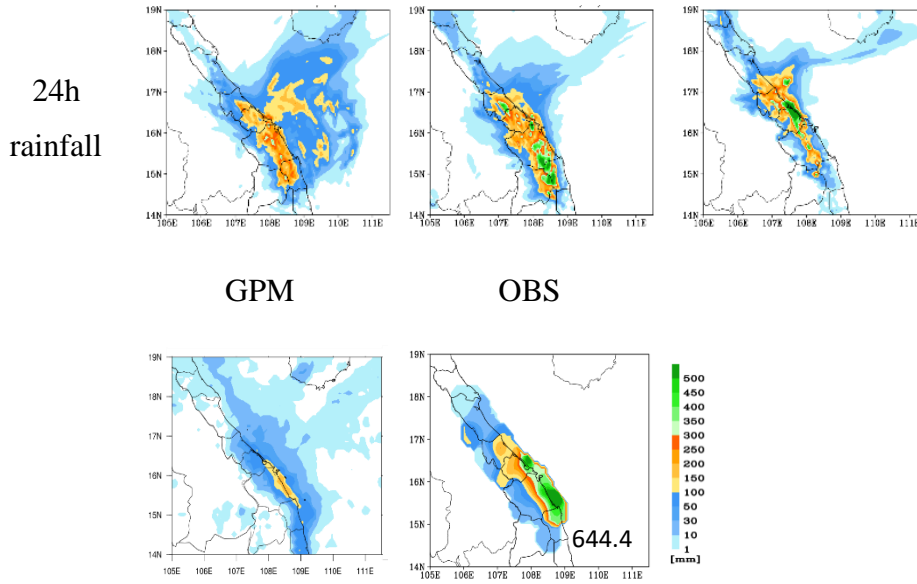
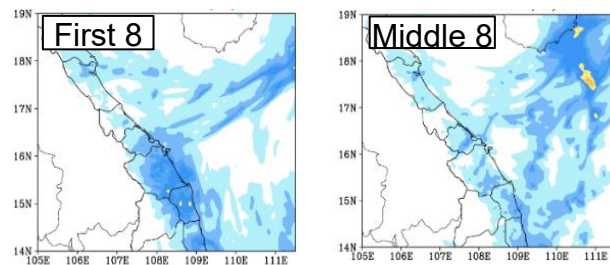


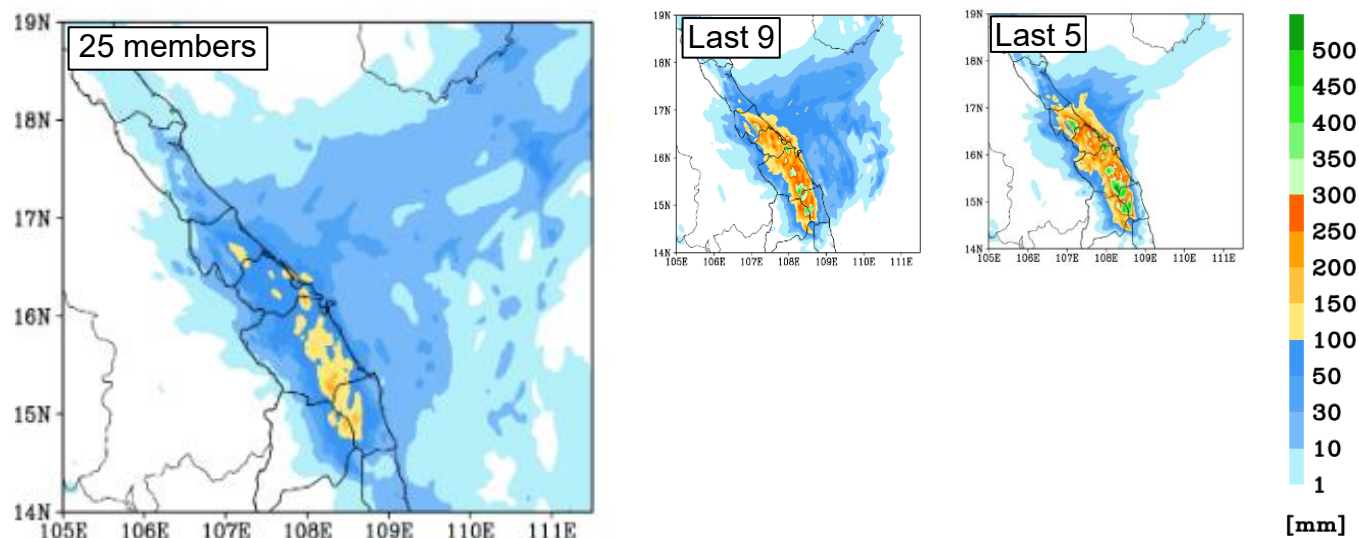
Figure 4. The predicted 24h rainfall by subgroup members, 24h accumulated rainfall by the Global Precipitation Measurement (GPM) estimate (IMERG Final Run product), 24h observed rainfall (mm, peak amount labeled at the lower-right corner) for the period of 12:00 UTC 9 December – 12:00 UTC 10 December 2018 as labelled. The same color bar (lower right) is used for all panels.

Besides the evaluation on time-lagged results using batches of ~~successive~~ fixed number of successive runs (every 4 members) as presented above, this study also grouped the members using different ensemble sizes based on their behavior in order to better assess the temporal evolution of forecast uncertainty and event predictability as the lead time shortened. Particularly, ~~this study divided~~ the 25 members were divided into several subgroups as shown in Fig. 5, including the first eight members (those executed during 12:00 UTC 3–06:00 UTC 5 December), the middle eight members (runs between 12:00 UTC 5 and 06:00 UTC 7 December), the last nine members (12:00 UTC 7–12:00 UTC 9 December), and the last five members (12:00 UTC 8–12:00 UTC 9 December), respectively. In other words, the last five members were those executed within 0–24 h (1 day) prior to the beginning of the target period, and so on.

In Fig. 5, it is clear that both the ensemble means from the last five and the last nine members compare quite favorably to the observation, not only in the accumulated amount but also in spatial distribution of rainfall. This indicates that the model could produce QPFs at fairly good quality and rather consistently since the time as early as roughly 48 h prior to the commencement of the rainfall event (also Fig. 3). These two sub-sub-ensemble groups within the short range gave much better quality in QPFs than the other sub-groups executed before them at longer lead times, including the first eight, middle eight, and all 25 members.

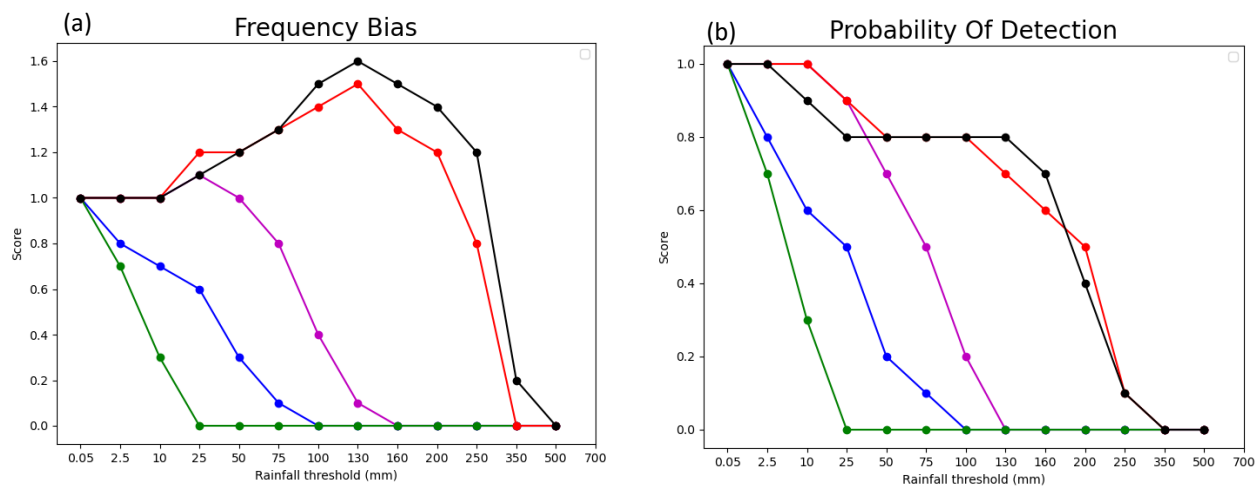
-In terms of skill scores, for example, the mean QPF by the last five members have TS = 0.4, POD = 0.8, FBS = 1.5, and FAR = 0.5 at 100 mm (per 24 h), while the last nine members give similar scores of TS = 0.5, POD = 0.8, FBS = 1.4, and FAR = 0.5 (Figs. 6a-d), respectively. On the contrary, the mean QPFs from both the first and middle eight and first-eight members only yield zero scores in TS, POD, and FBS with no skill in FAR at 100 mm (and above), obviously due to not enough rainfall in central Viet Nam in most of their members. At 200 mm (per 24 h), similarly, the last five members (TS = 0.2, POD = 0.4, FBS = 1.4, and FAR = 0.7) and the last nine members (TS = 0.3, POD = 0.5, FBS = 1.2, and FAR = 0.6) again produce much better scores in QPFs, compared to no skill in all four scores in QPFs from the middle eight, first eight, and all 25 members (Figs. 67a-d). In SSS, the mean from the last nine members exhibits the highest score (0.64), the middle eight members have the lowest score (0.04), and the mean from all 25 members is 0.43 (Fig. 6e).





475

476 **Figure 5.** Ensemble mean rainfall (shaded, scale on the right) from all 25 time-lagged
 477 members, executed every 6 h from 12:00 UTC 3 December to 12:00 UTC 9 December, for
 478 the 24h period from 12:00 UTC 9 December to 12:00 UTC 10 December.



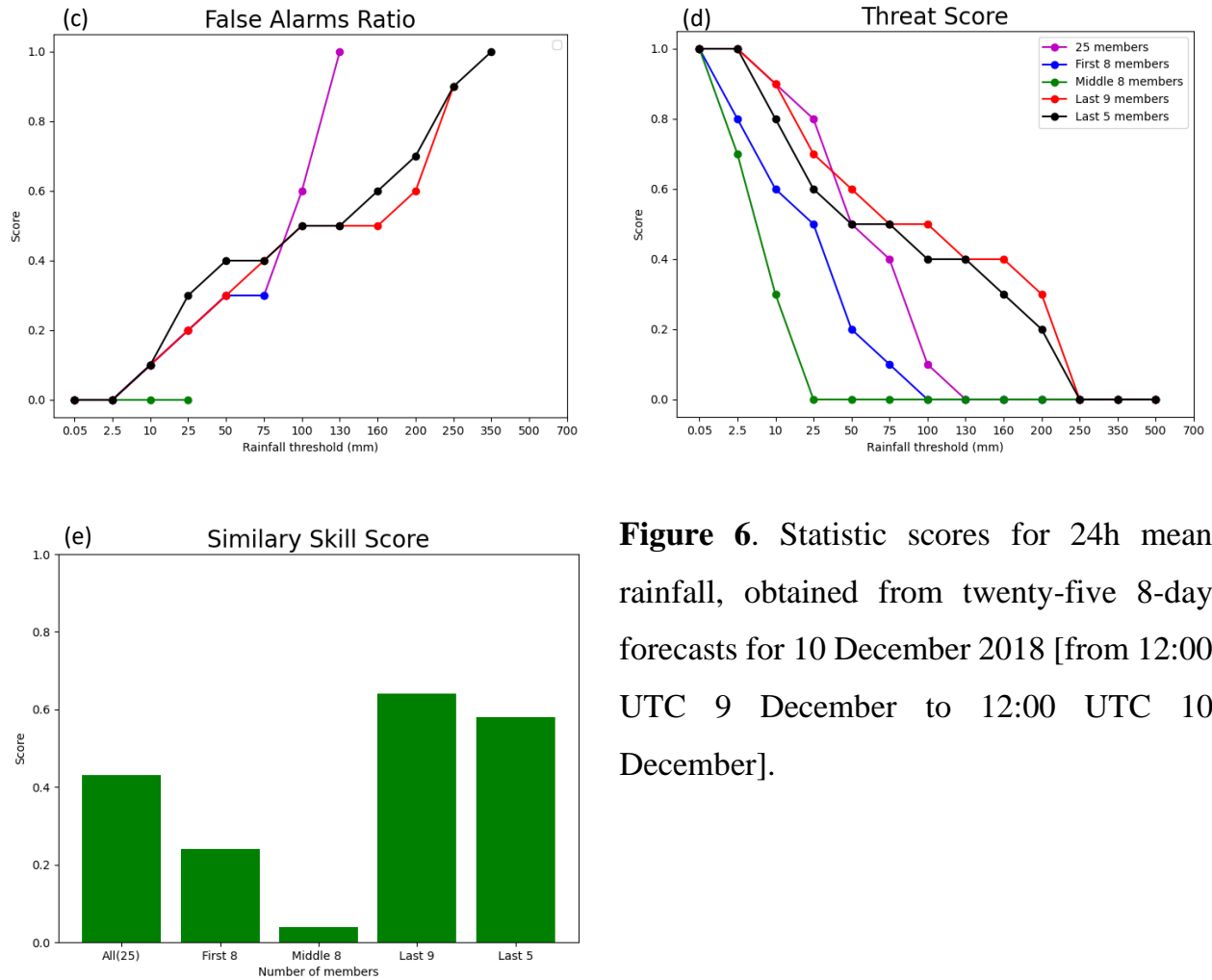


Figure 6. Statistic scores for 24h mean rainfall, obtained from twenty-five 8-day forecasts for 10 December 2018 [from 12:00 UTC 9 December to 12:00 UTC 10 December].

479

480 However, as indicated by the SD, the spreads in rainfall scenarios in both ensembles from
 481 the last five and nine members are quite large (Fig. 7). Thus, while the lagged members
 482 can produce a wide range of possible rainfall scenarios for the D18 event, which is the
 483 main purpose of an ensemble as reviewed [in](#) (Section 1), the members often cannot agree
 484 on the precise locations of heavy rainfall. Given the small scale of local convection during
 485 the event, this result is perhaps anticipated. On the other hand, the maxima in spread are
 486 >160 mm in Fig. 7 among the last nine members, ~~perhaps quite~~ and reasonable in magnitude
 487 compared to the peak amount~~ss~~ of about 400 mm in the ensemble mean. In any case, Figs.
 488 6 and 7 indicate that the predictability of the D18 event changed considerably with time,

and the 2.5-km CReSS has a good skill in QPFs inside the short range (≤ 72 h). However, it remains difficult to predict the event successfully at longer lead times.

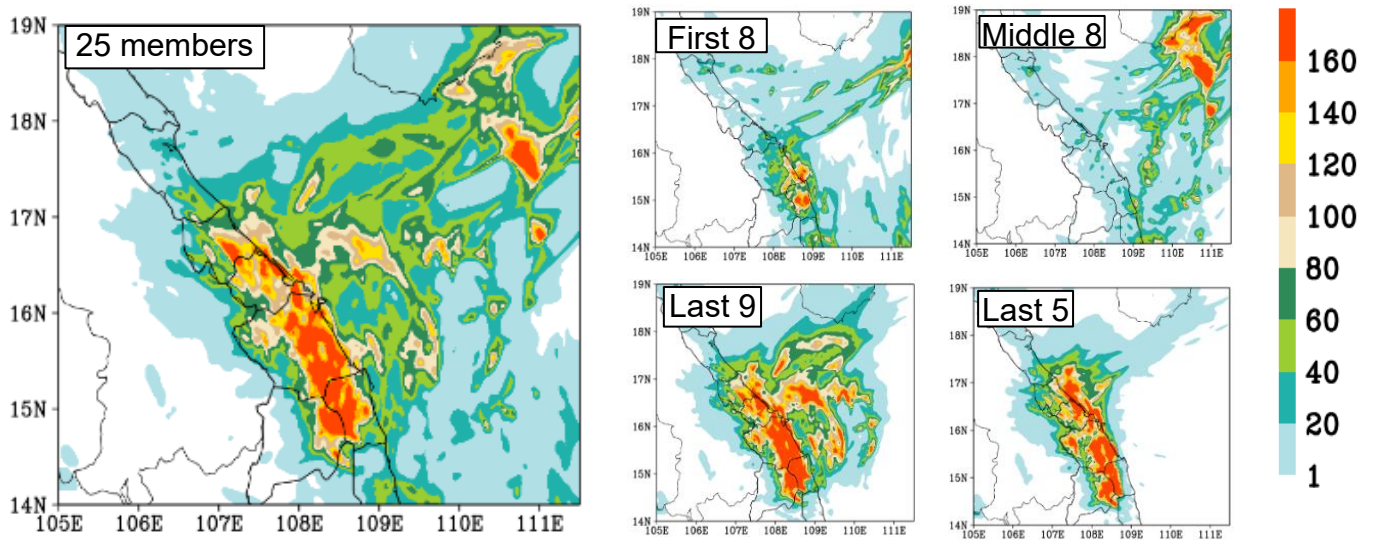
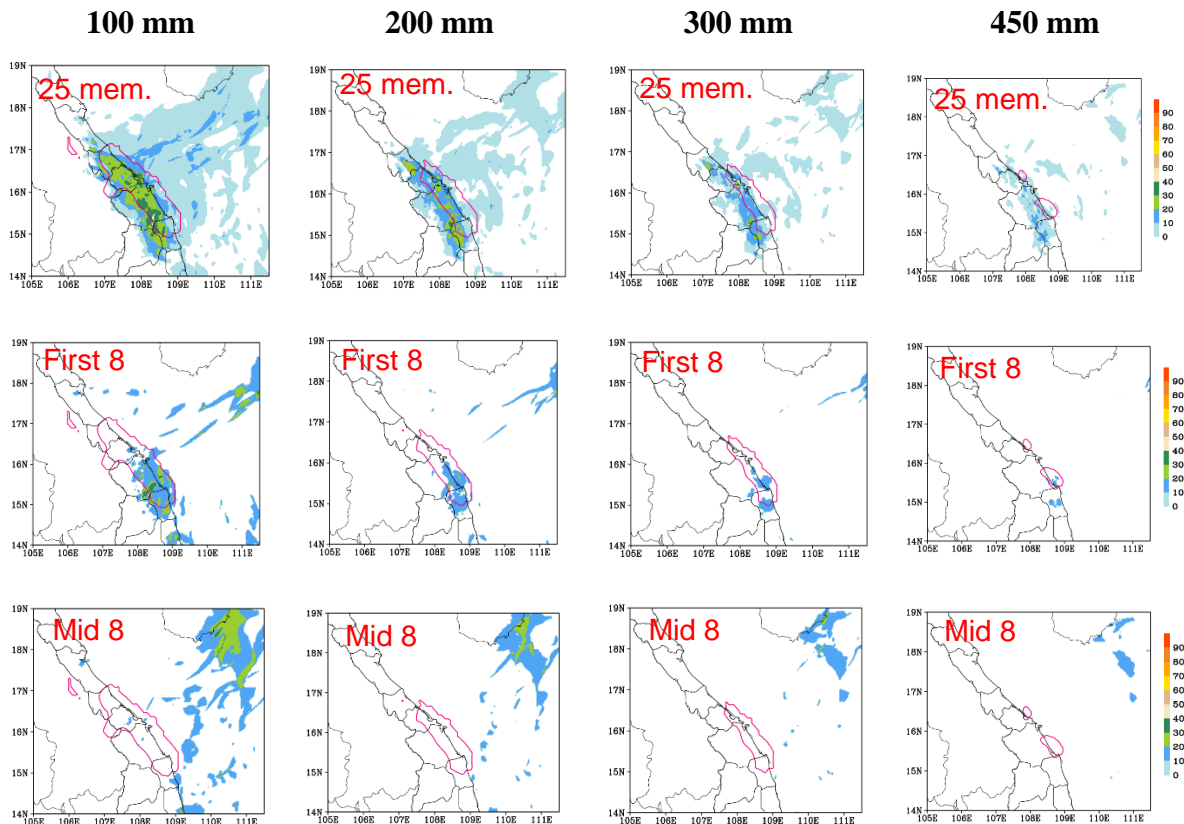


Figure 7. The spread (shaded, scale on the right) from all 25 time-lagged members, executed every 6 h from 12:00 UTC 3 December to 12:00 UTC 9 December, for the 24h period from 12:00 UTC 9 December to 12:00 UTC 10 December.

The probability information derived from the sub-ensemble groups at four different rainfall thresholds from 100 to 450 mm is shown in Fig. 8, in which the increase in heavy-rainfall probability in central Viet Nam and thus the predictability of the event with time is also evident. From the first eight members executed at the longest range (≥ 102 h prior to rainfall accumulation), there is only a 10-25% chance in parts of central Viet Nam to receive at least 100 mm of rainfall for 10 December (from 12:00 UTC 9 to 12:00 UTC 10 December). The probability is even lower from the middle eight members (run between 54-96 h prior to target period), as their SSS is the lowest among all sub-ensemble groups and only a

couple of the runs could reach 100 mm anywhere inland in central Viet Nam. As the lead time shortens to inside the short range, the probabilities to have ≥ 100 mm of rainfall increase dramatically, to roughly 70-80 % in the last nine members and further to over 80-90% in the last five members. Due to the contribution from later members, about 20-40% of all 25 members can reach 100 mm inland. Toward higher thresholds, the probabilities decrease in Fig. 8 as expected, so ~~do are~~ the areal sizes actually reaching those thresholds (~~red pink~~ contours). At the highest value of 450 mm, the ensembles in general show less than about 20% ~~and~~ 30% chances for its occurrence from the last five and last nine members, respectively, and the high probability areas are also slightly more inland than the observed one.



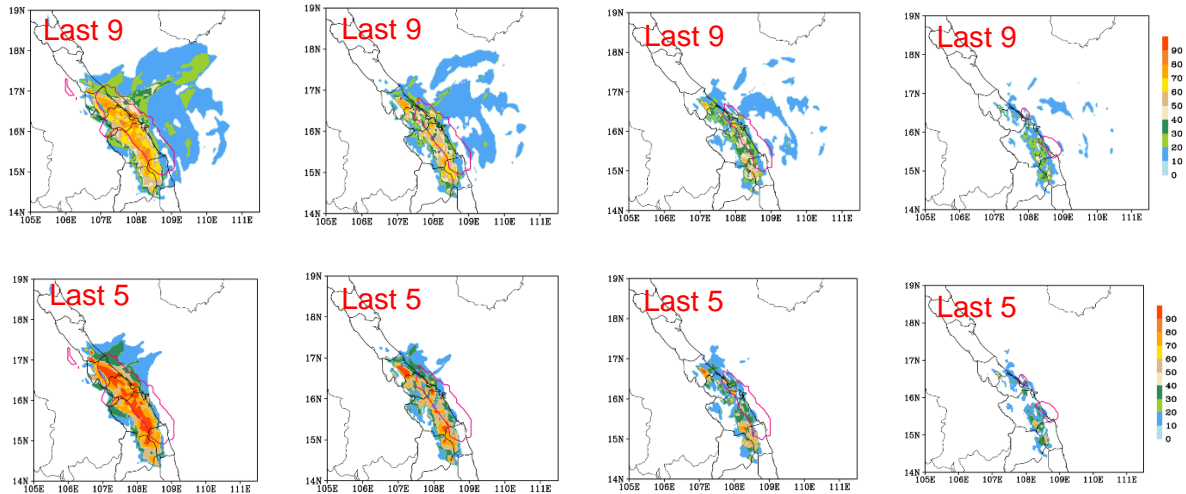


Figure 8. Probability distribution (%; shaded, scale on the right) from all 25 time-lagged members, executed every 6 h from 12:00 UTC 3 December to 12:00 UTC 9 December, reaching thresholds of 100, 200, 300, and 450 mm, for the 24h period from 12:00 UTC 9 December to 12:00 UTC 10 December. The observed areas at the same thresholds are depicted by the pink contours. For each picture, red labeled at the top-left corner show the number of members grouped to calculate the probability distribution.

3.2 Ensemble-based sensitivity analysis

The results in [Sectionpart 3.1](#) above reveal that the CReSS model with a horizontal [grid size](#) resolution of 2.5 km [predicted](#) had good well QPFs [for](#) predicted the rainiest day of the event [and performed better than those](#) while other reviewed in [Section 1](#) models can't capture it. Therefore, [this part was made](#) relying on this good performance, the ESA is carried out in this subsection.

Firstly, [five good members](#) (those with initial times at 18:00 UTC on 4, 00:00, 06:00, and 12:00 UTC on 8, and 00:00 UTC on 9 December) and five bad ones (those ran at 18:00 UTC on 3, 18:00 UTC on 5, 06:00 and 18:00 UTC on 6, and 06:00 UTC on 7 December) are chosen and by using their differences (good minus bad members), [Fig.ure 9](#) showsn that the main reason for the significantly different forecast outcomes [lies in](#) between five good members (those with initial times at 18:00 UTC on 4, 00:00, 06:00, and 12:00 UTC on 8, and 00:00 UTC on 9 December) and five bad ones (those ran at 18:00 UTC on 3,

18:00 UTC on 5, 06:00 and 18:00 UTC on 6, and 06:00 UTC on 7 December)(good minus bad members), is that there are significant differences in the input datasets (i.e., IC/BCs). Specifically, the surface easterly winds were much stronger and the relative humidity much higher surrounding central Viet Nam and its upstream areas in the GFS forecast data valid at 12:00 UTC on 9 December (used as BCs in CReSS runs) in the good members than in the bad ones (Fig. 9a). Subsequently, the good CReSS members produced much more rainfall in central Viet Nam (Fig. 9b). These factors were also identified as crucial for the extreme rainfall in the D18 event in Part 1, ~~and thus the good CReSS members produced much more rainfall in central Viet Nam (Fig. 9b).~~

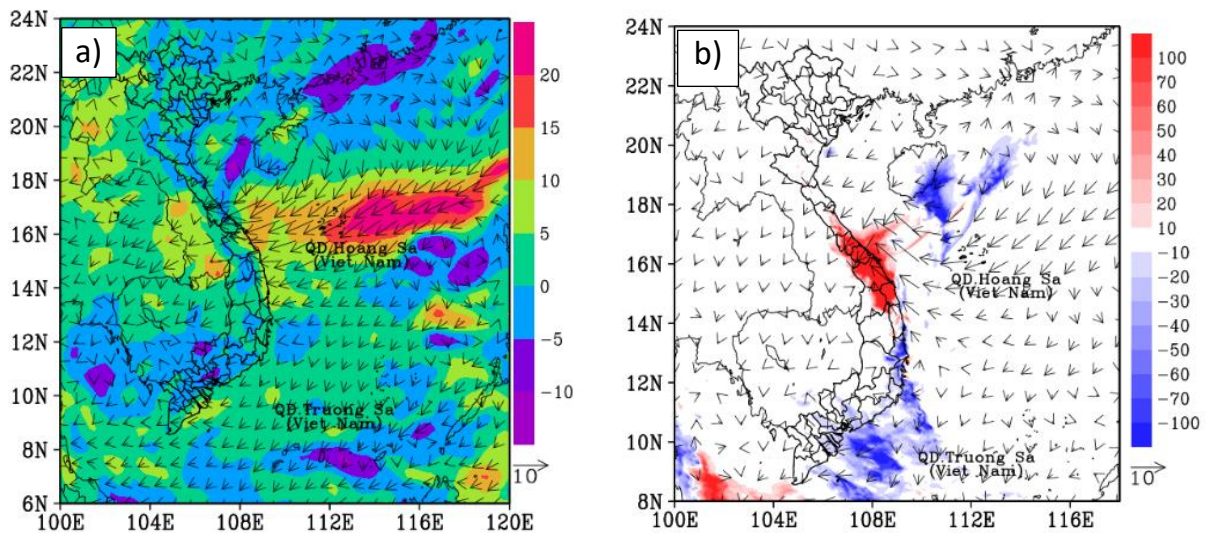
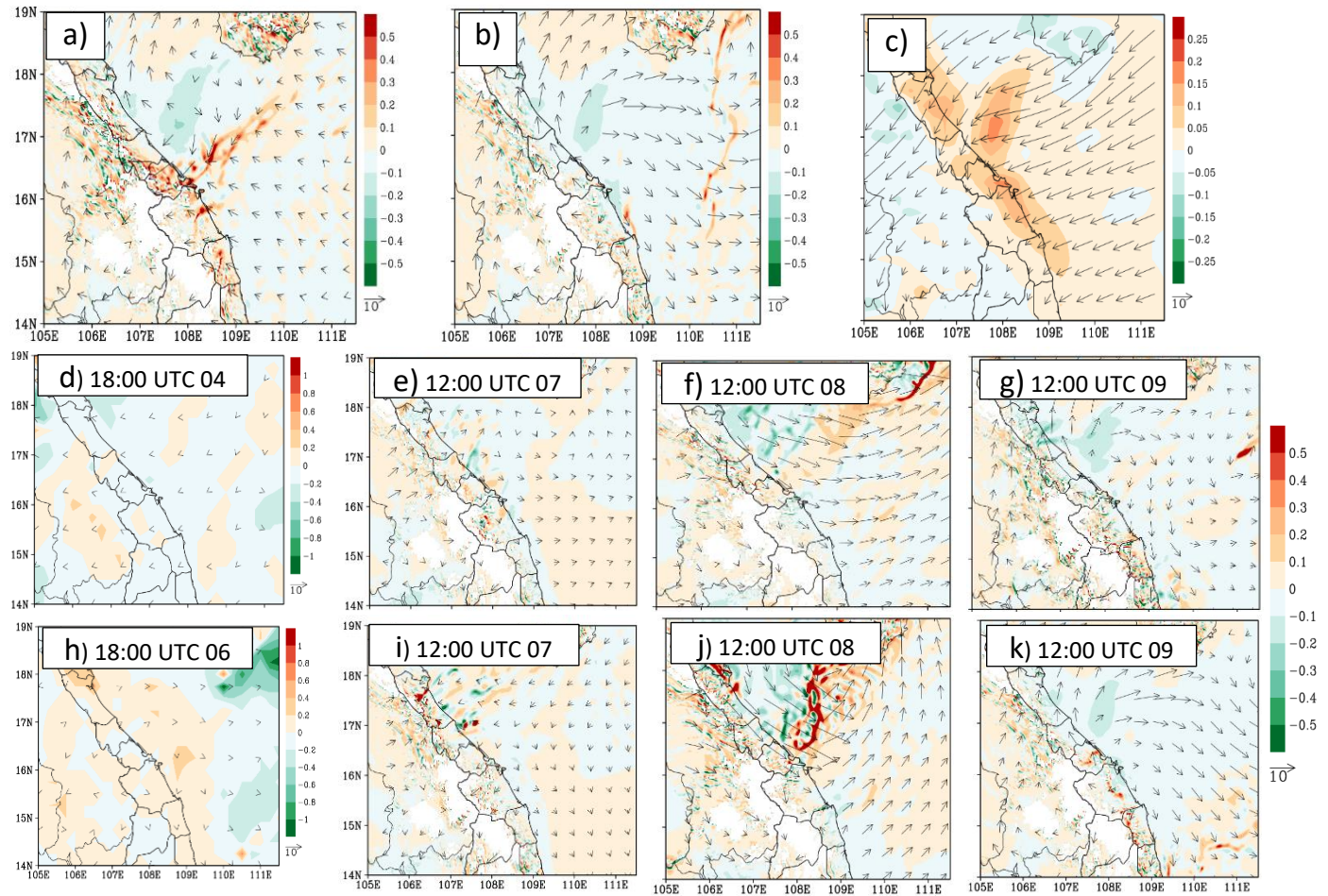


Figure 9. The difference in (a) input data (boundary conditions) and (b) CReSS output between averaged 5 good members (members ran at 18:00 UTC 4, 00:00 UTC 8, 06:00 UTC 8, 12:00 UTC 8, 00:00 UTC 9) and 5 bad members (members ran at 18:00 UTC 3, 18:00 UTC 5, 06:00 UTC 6, 18:00 UTC 6, 06:00 UTC 7). For input data, relative humidity (% , shaded) and surface wind (ms^{-1} , vector) at 12:00 UTC December 9 2018. For CReSS output, 24-h accumulated rainfall (mm, shaded) and surface wind (ms^{-1} , vector).

Meanwhile, Fig. 10 shows the difference in the evolution of synoptic-scale patterns (features), ~~with a zoomed into~~ the study area. To be more specific, Fig. 10a

~~depicts~~shows the difference (~~CReSS~~model output ~~-minus~~ NCEP FNL analysis~~-data~~) in the horizontal wind and vertical velocity between ~~the~~ averages ~~of the~~ 5 good members and the NCEP FNL analysis~~-data~~ at 925 hPa ~~and~~ at 12:00 UTC 09, ~~and it~~ is small although each member was initialized at ~~a~~ different lead time. It implies that these members captured well the evolution of weather patterns of this event. Additionally, the model vertical velocity is ~~seen to be~~observed ~~stronger~~greater than ~~the~~ NCEP FNL ~~data~~analysis~~-data~~. Therefore, these members produced the rainfall closer to ~~the~~ observation ~~with the presence of complex terrain in~~ed rainfall~~-even~~ the study area ~~is a complex terrain~~. ~~On the contrary~~Contrarily, bad members ~~did not~~ ~~poorly~~captured the evolution of weather patterns ~~well enough~~ (Fig. 10b), ~~and~~. ~~Consequently,~~ ~~these members could not~~an't produce ~~good QPFs as a result~~rainfall close to the observed rainfall data.

Furthermore, Figs. 10d indicates ~~very small~~ ~~the~~ differences in ~~the IC~~initial~~-data~~ of the member that ~~was~~ initialized at 18:00 UTC 04 ~~to the FNL analysis (thus suggesting smaller errors)~~is very small, especially over the study area. ~~From this initial data,~~ ~~t~~The evolution of weather patterns ~~in this CReSS run also agreed well with the analyses every 24 hours based on this initial data is also observed small during the~~at first ~~three~~3 days- (not shown), ~~and the differences remained relatively small lead time. The difference then developed larger. However, the difference is smaller even~~ at 12:00 UTC 09, ~~at a lead time of (roughly~~approximate 5 days ~~lead time)~~-(Figs. 10e,f,g). Compare to this, ~~the~~ bad member initialized at 18:00 UTC 06 (~~at a shorter lead time by 2~~-days~~-lead time shorter~~) ~~exhibited~~have ~~somewhat a~~larger differences in the ~~initialized~~ state ~~in relation to the NCEP FNL analysis~~of atmosphere, ~~even this difference is also small in comparison with NCEP FNL analysis data~~ (Fig. 10h). ~~t~~This difference then led to ~~a~~larger ~~and more evident~~ differences in~~-evolution of~~ weather patterns, as ~~seen in~~observed~~-at~~ Figs. 10 i, j, ~~and k~~by ~~this particular~~a bad member that performed worse in QPFs (member ran at 18 UTC 06). The ~~results here~~se not only indicate that it is still possible to have good ~~rainfall~~ forecasts at a lead time~~-of~~ up to 5 days, but also show ~~some predictability by a cloud-resolving model~~



at such long lead times the good performance of CReSS in predictability of the event at longer lead time.

Figure 10. The difference in the horizontal wind (ms^{-1} , vector, reference length at the low-right corner of the panel), and vertical velocity (ms^{-1} , shaded, the reference color scale is on the right of panel) between (a) averaged 5 good members and (b) averaged 5 bad members and the NCEP FNL analysis data at 925 hPa and at 12 UTC 09. (c) The NCEP FNL analysis horizontal wind (ms^{-1} , vector, reference length at the low-right corner of the panel) and vertical velocity (ms^{-1} , shaded) at 925 mb and at 12 UTC 09. (d) The difference in the horizontal wind (ms^{-1} , vector, reference length at the low-right corner of the panel),

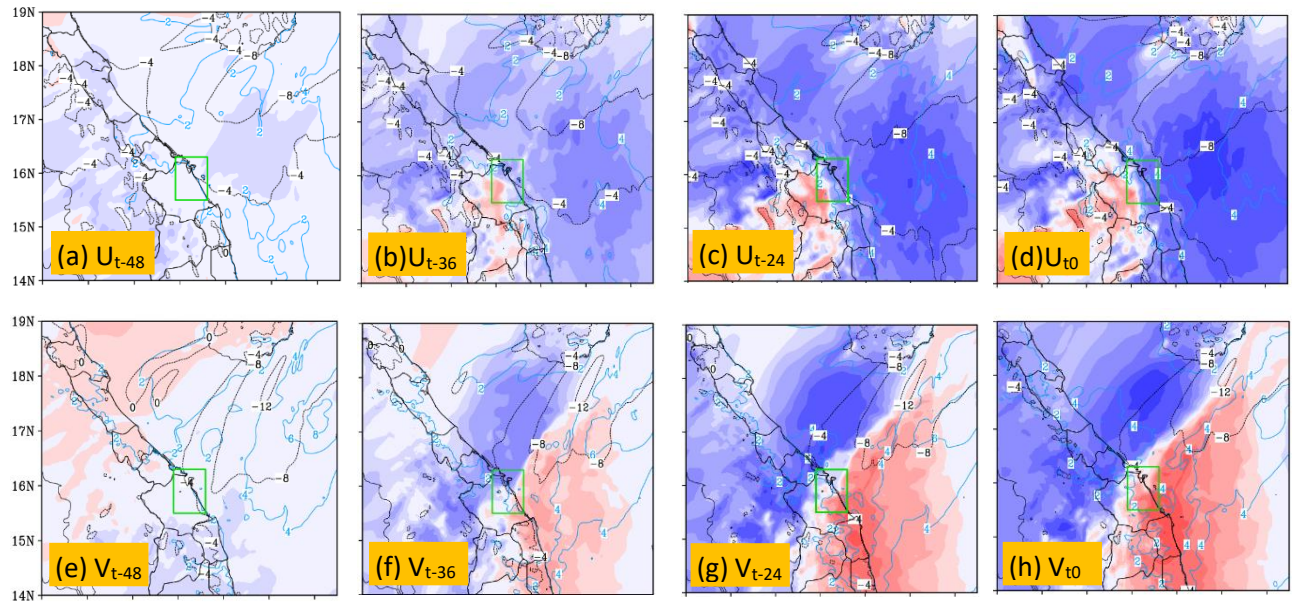
and relative humidity (% , shaded, the reference color scale is on the right of panel) between the initial data of a good member at a longer lead time (at 1800 UTC 4 Dec) and the NCEP FNL analysis data at 925 hPa. (e), (f), and (g) present the difference in the evolution of weather features with time by this good member. (h) as in (d) but for a bad member (member ran at 1800 UTC 6 Dec). (i), (j) and (k) as in (e), (f), and (g), respectively, but for mentioned bad member.

~~, (i), (j), and (k) by a bad member (member ran at 18 UTC 05).~~ Compared variables are horizontal wind at 925 hPa (ms^{-1} , vector, reference length at the low-right corner of the panel) and vertical velocity (ms^{-1} , shaded, the reference color scale is on the right of panel) The NCEP FNL analysis horizontal wind (ms^{-1} , vector, reference length at the low-right corner of the panel) and vertical velocity (ms^{-1} , shaded) at 925 mb and ~~at 12 UTC 09.~~

Additionally, the above resultse also reaffirm that ~~a~~very small differences in the ~~initial~~initialized data ~~can~~ould then lead to a ~~vastly~~very different ~~in the~~ outcome, especially as the forecast range increases, in extreme rainfall events (such as the D18 event) that involve highly nonlinear deep convection. ~~On the other hand, the predicted rainfall is very sensitive with every small difference in the initial data. Besides, a~~s pointed out in Part 1, ~~that~~ the low-level wind convergence led to moisture convergence and these conditions played a crucial role in~~resulted in~~ the D18 event. ~~T~~And the southward movement of the low-level wind convergence also dictated the movement of ~~heavy~~ the convective rainband during the event. Therefore, the ESA was applied on relevant variables, including the horizontal~~the zonal and meridional components of~~ wind, and ~~water~~ mixing ratio of water vapor. The quantitative results are shown in Figs. 11-13 and presented below.

~~To be more specific,~~ Figure 11 shows the sensitivity of mean 24-h total rainfall inside the green box in central Viet Nam (R) to zonal (u) and meridional (v) wind components and water vapor mixing ratio (q_v) at the ~~-~~surface, with ~~and~~ the ensemble mean ~~are~~ also plotted.

It is clear that the sensitivity of rainfall to these variables is lower at longer forecast ranges and becomes higher as the lead time ~~shorten~~ ~~lead times~~. Specifically, from two days before (t_{-48}) to the starting time of the accumulation period (t_0), the sensitivity of rainfall to u -wind over the SCS and along the coast of central Viet Nam turned more negative, indicating heavier rainfall associated with stronger easterly winds ($u < 0$) near the surface, especially in areas immediately upstream atoward t_0 (Figs. 11a-d). The rainfall's sensitivity to v -wind leading to t_0 , on the other hand, exhibited a dipole structure in pattern, with negative values to the north-northwest and positive values to the south-southeast across central Viet Nam and the upstream ocean (Figs. 11e-h). This structure indicates a stronger confluence in northeasterly winds over the region in rainier members, consistent with the results in Part 1. In Figs. 11e-h, the increase in v -wind just south of central Viet Nam is particularly evident, from -10 mm (per SD; $(SD = 2 \text{ ms}^{-1})$ at t_{-48} to over $+70$ mm (per SD ~~– (Standard deviation, SD = 2–4 ms⁻¹)~~ at t_0 . Thus, the precipitation amount overin the D18 event in central Viet Nam in the D18 event is highly sensitive to the strength and confluence of northeasterly winds near the surface in short-range forecasts-forecasts. Similarly, the rainfall was- also highly sensitive to the water vapor amount and its flux convergences shown in (Figs. 11i-l).



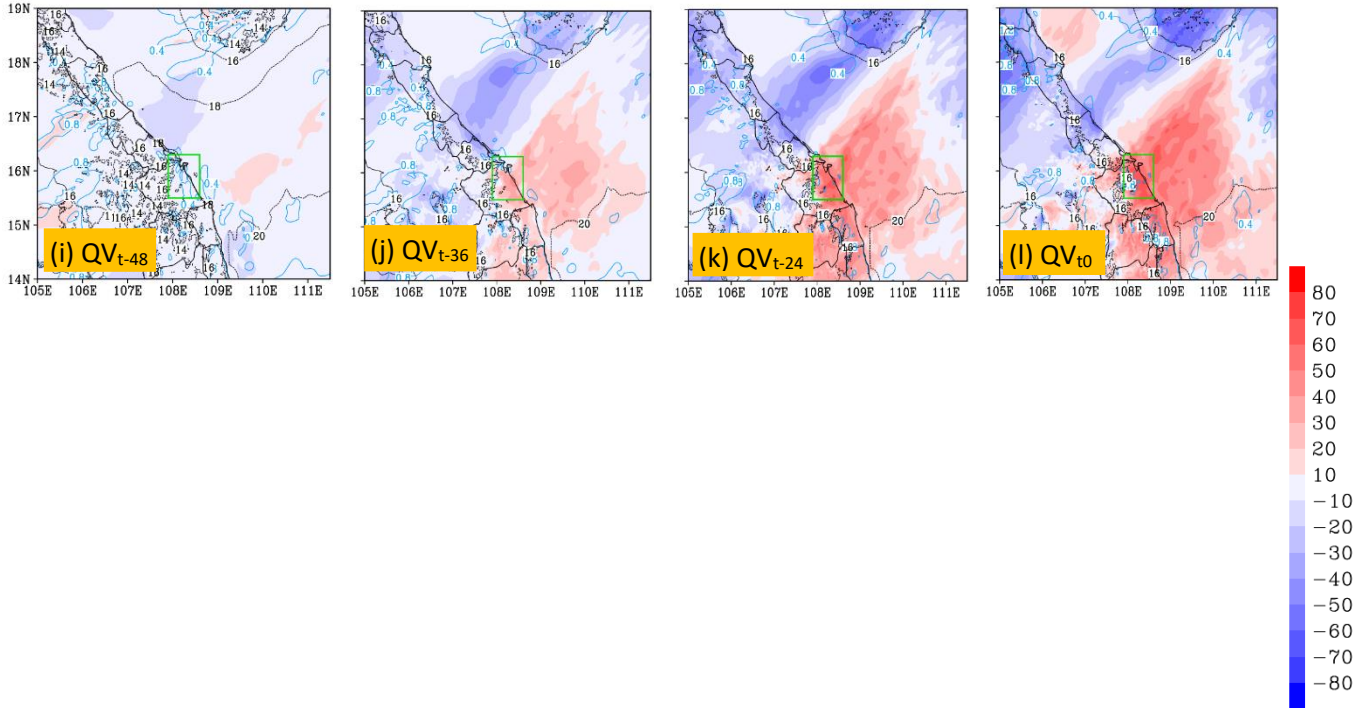
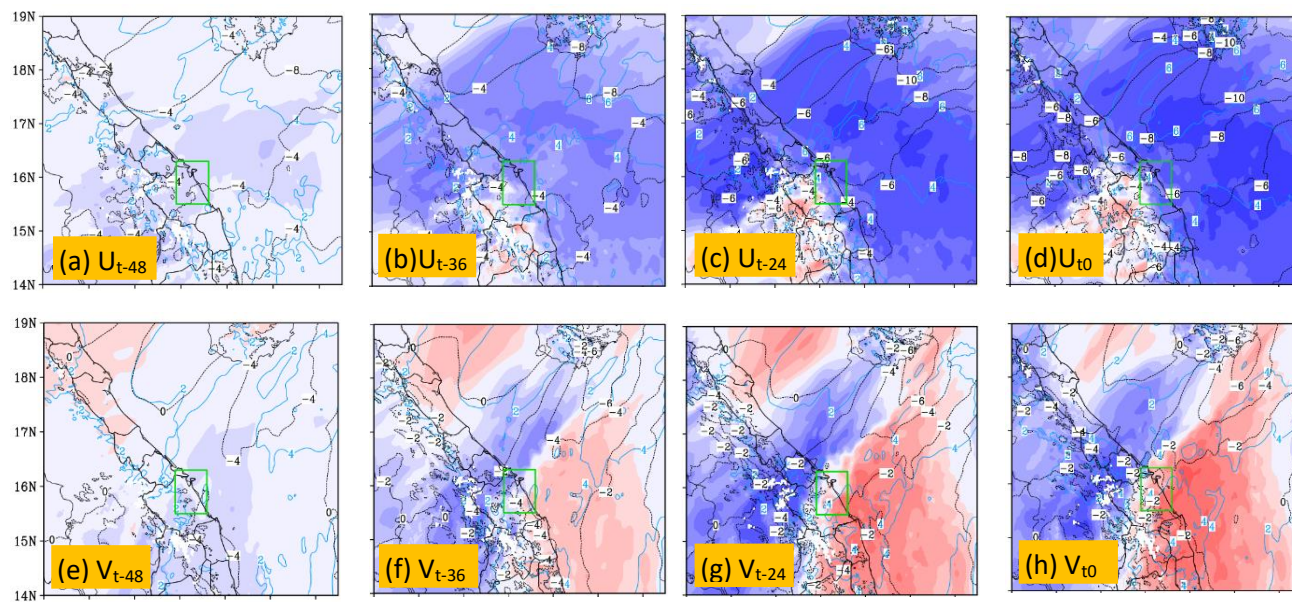


Figure 11. The sensitivity (mm, per SD, color, scale on the right) of areal-mean 24h accumulated rainfall in central Viet Nam starting from t_0 (i.e., R, averaging area depicted in green box) to surface wind components (ms^{-1} , shaded) and the ensemble mean (contours, every 4 ms^{-1}) and to surface water vapor mixing ratio (r , g kg^{-1}) and its ensemble mean (contours, every 0.06 g kg^{-1}) at different times at 24h intervals from (a) t_{-48} to (f) t_0 . The time of t_0 is 12:00 UTC 9 December 2018. In which, (a), (b), (c), (d) for the zonal wind component. (e), (f), (g), (h) for the meridional wind component, and (i), (j), (k), (l) for surface water vapor mixing ratio. The standard deviation is exhibited by the medium blue contours.

Slightly higher up at 1476 m (near 850 hPa), where easterly flow prevailed during the D18 event (see Fig. 3b in Part 1), the sensitivity of rainfall to u and v winds exhibits similar spatial patterns (Figs. 12a-h) to those at the surface (Figs. 11a-h), with stronger easterly winds and larger confluence in association with heavier rainfall. Similarly, the rainfall- in central Viet Nam is still ~~still~~ shows -highly-igh sensitive to mixing ratio at this level, both locally and over the surrounding area scale -in central Viet Nam at this level (Figs. 12i-l), again especially at shorter lead times. At the local scale, Presumably, this positive

correlation presumably is linked ~~due~~ to upward transport of moisture, as the ascending motion in convective clouds could become larger at this level (and also more vigorous in rainier members).



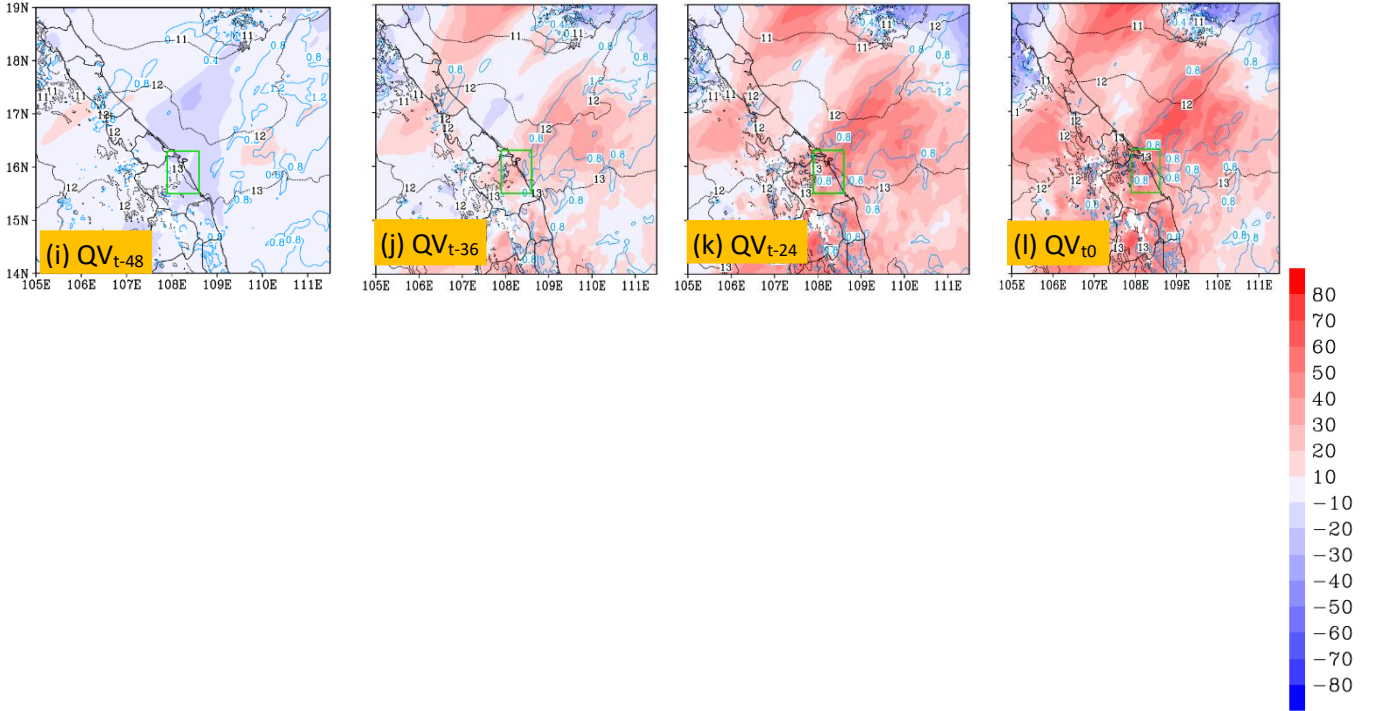
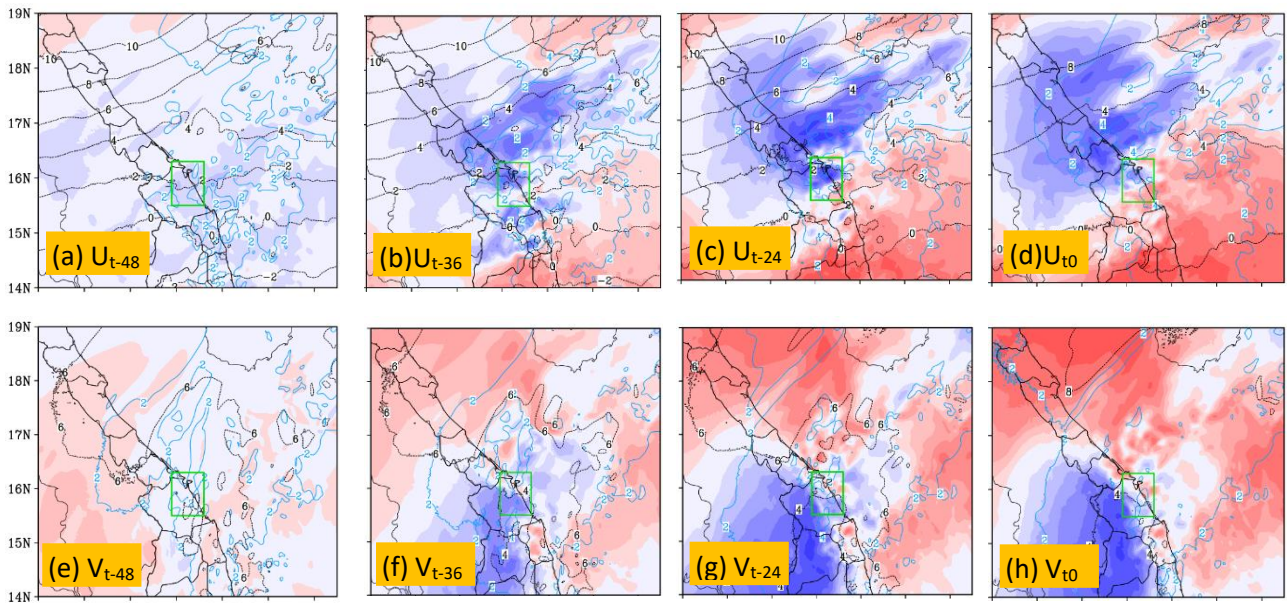


Figure 12. The sensitivity (mm, per SD, color, scale on the right) of 24h accumulated rainfall in central Viet Nam starting from t_0 (i.e., R, averaging area depicted in green box) to the wind components (ms^{-1} , shaded) and the ensemble mean (contours, every 2 ms^{-1}) and to water vapor mixing ratio (r , g kg^{-1}) and its ensemble mean (contours, every 0.4 g kg^{-1}) at attitude of 1476 m and at different times at 24h intervals from (a) t_{-48} to (f) t_0 . The time of t_0 is 12:00 UTC 9 December 2018. In which, (a), (b), (c), (d) for the zonal wind component. (e), (f), (g), (h) for the meridional wind component, and (i), (j), (k), (l) for water vapor mixing ratio. The standard deviation is exhibited by the medium blue contours.

At the upper level of 5424 m (near 500 hPa), it is seen that from t_{-48} to t_0 , dipole structures developed in the sensitivity patterns of rainfall to both u and v winds (Figs. 13a-h). To u winds, positive sensitivity up to about $+70 \text{ mm (per SD; (SD = } 2\text{-}4 \text{ ms}^{-1} \text{ dependings on } t_*)$ existed to the south, with-and negative valuessensitivity up to $-70 \text{ mm (per SD; (SD = } 2\text{-}4 \text{ ms}^{-1} \text{ depends on } t_*)$ to the north of central Viet Nam. Meanwhile, positive sensitivity to v -wind appeared to the north and east with negative sensitivity to the south and west of the rainfall area. AsWhile the prevailing winds at 500 hPa were southeasterliesy over southern

Viet Nam and southwestern ~~iesy~~ over northern Viet Nam during the D18 event (thus with
 anticyclonic curvature, see Fig. 3c in Part 1), the above sensitivity patterns, already
 apparent at t_{-24} ~~already~~, (Figs. 13c,g), corresponded to stronger diffluence/divergence and
 a weaker anticyclone aloft to favor more rainfall. To q_v , positive sensitivity signals up to
 +70 mm (per SD; $(SD = 1.2 \text{ g kg}^{-1})$) also appeared over the rainfall area at t_{-24} and t_0 (Figs.
 13i-l), and the reason is similar to ~~that~~ those near 850 hPa in Fig. 12. Overall, the ESA
performed in this study ~~se ensemble-based sensitivity analyses~~ indicated clearly that the
 synoptic pattern that caused the D18 event already developed at times more than 24 h
 earlier, and this explains why, with a high enough resolution and cloud-resolving
 capability, the CReSS forecasts could better predict and improve the QPFs inside the short
 range as shown in Section 3.



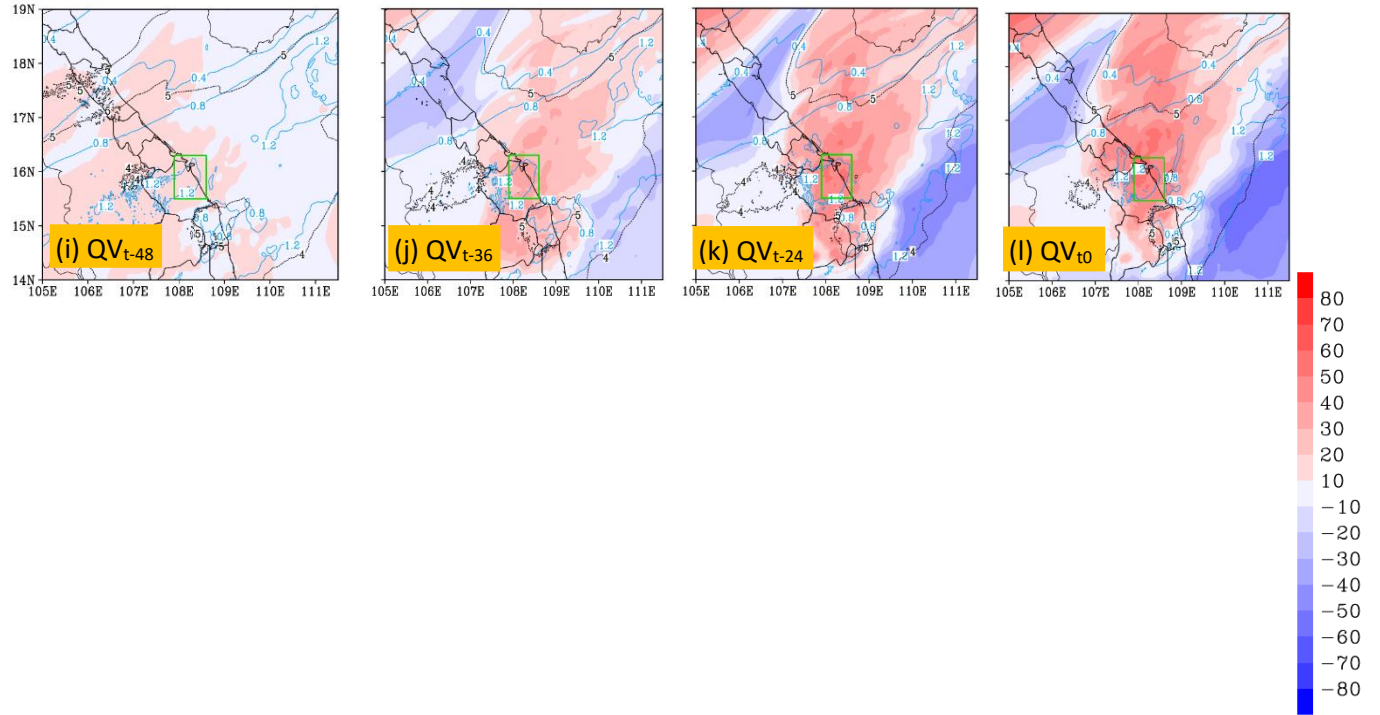


Figure 13. The sensitivity (mm, per SD, color, scale on the right) of 24h accumulated rainfall in central Viet Nam starting from t_0 (i.e., R, averaging area depicted in green box) to the wind components (ms^{-1} , shaded) and the ensemble mean (contours, every 2 ms^{-1}) and to water vapor mixing ratio (r , g kg^{-1}) and its ensemble mean (contours, every 0.4 g kg^{-1}) at attitude of 5424 m and at different times at 24h intervals from (a) t_{-48} to (f) t_0 . The time of t_0 is 12:00 UTC 9 December 2018. In which, (a), (b), (c), (d) for the zonal wind component. (e), (f), (g), (h) for the meridional wind component, and (i), (j), (k), (l) for water vapor mixing ratio. The standard deviation is exhibited by the medium blue contours.

~~These ensemble-based sensitivity analyses indicated clearly that the synoptic pattern that caused the D18 event already developed at times more than 24h earlier.~~

4 Conclusion

As high resolution is required in numerical models to predict heavy rainfall more successfully, the present work utilizes a time-lagged high-resolution ensemble forecast system and evaluates how well the D18 event (during 9-12 December 2018) in central Viet Nam can be predicted in advance before its occurrence. Using the CReSS model with a

grid size of 2.5 km (912×900 in dimension with 60 vertical levels), ensemble forecasts were produced with a total of 29 time-lagged runs at 6-h intervals, each out to a forecast range of 192 h (eight days). Based on the goals raised from the analysis in Part 1, the key findings of this Part 2 study are summarized as follows:

The first goal of this study is regarding the scientific hypotheses that at a higher resolution, the cloud-resolving time-lagged ensemble can improve the QPFs of the D18 event at the short range, and may also be able to extend the lead time of decent QPFs beyond the short range. Our evaluation results confirm that this strategy using the CReSS model can effectively improve the QPFs of this event at the short range. Furthermore, the results also demonstrate that a decent QPF for 10 December (the rainiest day) can be made at a longer lead time (initialized at 1800 UTC 4 December), when good initial conditions are provided.

About the second goal, our investigation in predictability indicates that the 2.5-km system predicted the rainfall fields on 10 December during the event fairly well, including both the amount and spatial distribution, within the short range at lead times of day 1, 2, and 3. More specifically, the SSS of QPFs at these three ranges are about 0.4, 0.6, and 0.7, respectively, with fairly consistent results among successive runs that indicate a reasonable predictability, despite some spread and disagreement on the precise locations of heavy rainfall. The above good results are due to the model's capability to better predict the conditions in the lower troposphere such as the wind fields.

At lead times longer than three days, however, the predictability of the event is lowered due to a higher level of forecast uncertainty, and the quality of QPFs drops with significant under-prediction. Nevertheless, good QPFs are still possible occasionally. At lead time beyond six days, it is challenging to achieve a good QPF at thresholds greater than 100 mm even with a high-resolution model. This is presumably linked to the rapid evolution of atmospheric conditions during such an extreme event surrounding Viet Nam in a tropical environment. In the present study, a CRM is applied to forecast extreme rainfall in central Viet Nam for the first time. Although still with certain limitations, our results do indicate hope to predict such events successfully beforehand, at least within the short range.

Therefore, based on the present work, more studies on the predictability of extreme rainfall in Viet Nam are recommended in the near future.

~~The present study also performed an ensemble sensitivity analysis to identify the important factors that influenced the 24 h rainfall amount in central Viet Nam in the D18 event~~Regarding the third and final goal, ESA results shows that the rainfall is most sensitive to the wind conditions in the lower troposphere leading to the event, with more rain associated with stronger northeasterly to easterly winds and their confluence over central Viet Nam (and the upstream region). Similarly, the rainfall also shows strong sensitivity to the moisture amount, not only at the surface but also further aloft at the upper levels. Besides, ESA also indicates~~s~~ that the synoptic pattern that caused the D18 event already developed at timing earlier in the past. Furthermore, in the ESA, the finer-scale features (convection) are also seen to link to synoptic conditions in their background, implying that it is meaningful to apply ESA to control the perturbations in initial fields.

The key findings in this study underscore that both practical predictability and ESA are intertwined, influencing the design and evaluation of ensemble forecast systems, and potentially applicable to other extreme rainfall events in the same season in Vietnam.

Acknowledgements: This study was supported by the project “*Research on the application of the Cloud-resolving model integrated with the regional numerical model to a 6-hour accumulated quantitative precipitation forecast with 24-48 hours lead time for Mid-Central Viet Nam*”, which is funded by the Ministry of Natural Resources and Environment (MONRE) under grant no. TNMT.2023.06.07, and also by the National Science and Technology Council (NSTC) of Taiwan under grants MOST 111-2625-M-003-001, 111-2111-M-003-005 NSTC 112-2625-M-003-001, ~~and NMOSTC 113-2625-M-003-001~~, and NSTC 113-2111-M-003-001.

Code and data availability. The CReSS model used in this study and its user's guide are available at the model website at http://www.rain.hyarc.nagoya-u.ac.jp/~tsuboki/cress_html/src_cress/CReSS2223_users_guide_eng.pdf (last access: 6 July 2023; Tsuboki and Sakakibara, 2007). The TIGGE data and its information are available at <https://confluence.ecmwf.int/display/TIGGE/TIGGE+archive>. The NCEP GFS dataset and its description are available at <https://rda.ucar.edu/datasets/ds084.1/>. The NCEP FNL operational global gridded analysis data and its information is available at <https://rda.ucar.edu/datasets/d083003/#>.

Author contributions. **Duc Van Nguyen** prepared datasets, executed the model experiments, performed the analysis, and prepared the first draft of the manuscript. **Chung-Chieh Wang** also prepared the first draft and provided the funding, guidance and suggestions during the study, and they participated in the revision of the manuscript. **Kien Ba Truong** provided the funding and participated revising of the manuscript. **Thang Van Vu, Pham Thi Thanh Nga, and Pi-Yu Chuang** also participated in the revision of the manuscript.

Competing interests. The authors declare that they have no conflict of interest.

References

- Ancell, and Hakim, G. J.: Comparing adjoint- and ensemble sensitivity analysis with applications to observation targeting. *Mon. Wea. Rev.*, 135, 4117–4134, doi:10.1175/2007MWR1904.1, 2007.
- Cotton, W. R., Tripoli, G. J., Rauber, R. M., and Mulvihill, E. A.: Numerical simulation of the effects of varying ice crystal nucleation rates and aggregation processes on orographic snowfall. *J. Appl. Meteorol. Clim.*, 25, 1658–1680, 1986.
- Coleman, A. A., and Ancell, B. C.: Toward the improvement of high-impact probabilistic forecasts with a sensitivity-based convective-scale ensemble subsetting technique. *Mon. Wea. Rev.*, 148, 4995–5014, <https://doi.org/10.1175/MWRD-20-0043.1>, 2020.

- Deardorff, J. W.: Stratocumulus-capped mixed layers derived from a three-dimensional model. *Bound.-Lay. Meteorol.*, 18, 495–527, 1980.
- Hu, C.-C., and Wu, C.-C.: Ensemble sensitivity analysis of tropical cyclone intensification rate during the development stage. *J. Atmos. Sci.*, 77, 3387–3405, <https://doi.org/10.1175/JAS-D-19-0196.1>, 2020.
- Hoa, V. V.: Comparative study skills rain forecast the middle part and central highland of several global models (In Viet Nameese). *Viet Nam journal of Hydrometeorology*. V. 667 No. 07 (2016), 2016.
- Hohenegger, C., and Schär, C.: Predictability and error growth dynamics in cloud-resolving models. *J. Atmos. Sci.*, 64, 4467–4478, <https://doi.org/10.1175/2007JAS2143.1>, 2007.
- [Huffman, G. J., Bolvin, D. T., Braithwaite, D., Hsu, K., Joyce, R., Kidd, C., Nelkin, E.J., Sorooshian, S., Tan, J., Xie, P.: Algorithm Theoretical Basis Document \(ATBD\) Version 06: NASA Global Precipitation Measurement \(GPM\) Integrated Multi-Satellite Retrievals for GPM \(IMERG\). NASA/GSFC, Greenbelt, MD, USA, \[https://gpm.nasa.gov/sites/default/files/2020--05/IMERG_ATBD_V06.3.pdf\]\(https://gpm.nasa.gov/sites/default/files/2020--05/IMERG_ATBD_V06.3.pdf\), 2020.](#)
- Ikawa, M. and Saito, K.: Description of a non-hydrostatic model developed at the Forecast Research Department of the MRI, MRI Technical report 28, Japan Meteorological Agency, Tsukuba, Japan, ISSN: 0386-4049, 1991.
- Kerr, C. A., Stensrud, D. J. and Wang, X.: Diagnosing convective dependencies on near-storm environments using ensemble sensitivity analyses. *Mon. Wea. Rev.*, 147, 495–517, <https://doi.org/10.1175/MWRD-18-0140.1>, 2019.
- Kondo, J.: Heat balance of the China Sea during the air mass transformation experiment. *J. Meteorol. Soc. Jpn.*, 54, 382–398, https://doi.org/10.2151/jmsj1965.54.6_382, 1976.
- Leith, C. E.: Theoretical skill of Monte Carlo forecasts. *Mon. Wea. Rev.*, 102, 409–418, 1974.

- Lin, Y.-L., Farley, R. D., and Orville, H. D.: Bulk parameterization of the snow field in a cloud model. *J. Appl. Meteorol. Clim.*, 22, 1065–1092, 1983.
- Louis, J. F., Tiedtke, M., and Geleyn, J. F.: A short history of the operational PBL parameterization at ECMWF, in: *Proceedings of Workshop on Planetary Boundary Layer Parameterization*, 25–27 November 1981, Shinfield Park, Reading, UK, 59–79, 1982.
- Lorenz, E.N.: The predictability of a flow which possesses many scales of motion. *Tellus*, 21, 289–307. <https://doi.org/10.3402/tellusa.v21i3.10086>, 1969.
- Lorenz, E.N.: Atmospheric predictability as revealed by naturally occurring analogues. *J. Atmos. Sci.*, 26, 636–646, 1969.
- Murphy, J. M.: The impact of ensemble forecasts on predictability. *Quart. J. Roy. Meteor. Soc.*, 114, 463–493, 1988.
- Murakami, M.: Numerical modeling of dynamical and microphysical evolution of an isolated convective cloud – the 19 July 1981 CCOPE cloud. *J. Meteorol. Soc. Jpn.*, 68, 107–128, 1990.
- Murakami, M., Clark, T. L., and Hall, W. D.: Numerical simulations of convective snow clouds over the Sea of Japan: Two dimensional simulation of mixed layer development and convective snow cloud formation. *J. Meteorol. Soc. Jpn.* 72, 43–62, 1994.
- Melhauser, C., and Zhang, F.: Practical and intrinsic predictability of severe and convective weather at the mesoscales. *J. Atmos. Sci.*, 69, 3350–3371, doi:10.1175/JAS-D-11-0315.1, 2012.
- Nhu, D. H., Anh, N. X., Phong, N. B., Quang, N. D., and Hiep, V. N.: The role of orographic effects on occurrence of the heavy rainfall event over central Viet Nam in November 1999. *Journal of Marine Science and Technology*. V. 17, No. 4B(2017), 31–36, 2017.

Nielsen, E.R. and Schumacher, R.S.: Using convection-allowing ensembles to understand the predictability of an extreme rainfall event. Monthly Weather Review, 144, 3651–3676, 2016.

Segami, A., Kurihara, K., Nakamura, H., Ueno, M., Takano, I., and Tatsumi, Y.: Operational mesoscale weather prediction with Japan Spectral Model. J. Meteorol. Soc. Jpn., 67, 907–924, https://doi.org/10.2151/jmsj1965.67.5_907, 1989.

Surcel, M., Zawadzki, I., and Yau, M. K.: On the filtering properties of ensemble averaging for storm-scale precipitation forecasts. Mon. Wea. Rev., 142, 1093–1105, doi:10.1175/MWR-D-13-00134.1, 2014.

Son, B. M. and Tan, P. V.: Experiments of heavy rainfall prediction over South of Central Viet Nam using MM5 (In Vietnamese). Viet Nam Journal of Hydrometeorology., 4(580), 9–18, 2009.

Toan, T. N., Thanh, C., Phuong, P. T., and Anh, T. V.: Assessing the predictability of WRF model for heavy rain by cold air associated with the easterly wind at high-level patterns over mid-central Viet Nam (In Vietnamese). VNU Journal of Science: Earth and Environmental Sciences. v. 34, n. 1S, dec. 2018. ISSN 2588-1094. <https://js.vnu.edu.vn/EES/article/view/4328>, 2018.

Torn, R.D., Hakim, G.J.: Initial condition sensitivity of western Pacific extratropical transitions determined using ensemble-based sensitivity analysis. Mon. Weather Rev. 137, 3388–3406. <https://doi.org/10.1175/2009MWR2879.1>, 2009.

Tsuboki, K. and Sakakibara, A.: Numerical Prediction of HighImpact Weather Systems: The Textbook for the Seventeenth IHP Training Course in 2007, Hydrospheric Atmospheric Research Center, Nagoya University, Nagoya, Japan, and UNESCO, Paris, France, 273 pp., http://www.rain.hyarc.nagoya-u.ac.jp/~tsuboki/cress_html/src_cress/CReSS2223_users_guide_eng.pdf (last access: 1 May 2019), 2007.

869 Tuoi Tre news: [https://tuoitre.vn/mien-trung-tiep-tuc-mua-lon-14-nguoi-chet-va-mat-tich-](https://tuoitre.vn/mien-trung-tiep-tuc-mua-lon-14-nguoi-chet-va-mat-tich-20181212201907413.htm)
870 20181212201907413.htm (last access: 5 June 2024), 2018

871 Wang, C.-C.*, Kuo, H.-C., Yeh, T.-C., Chung, C.-H., Chen, Y.-H., Huang, S.-Y.,
872 Wang, Y.-W., and Liu, C.-H.: High-resolution quantitative precipitation forecasts and
873 simulations by the Cloud-Resolving Storm Simulator (CReSS) for Typhoon Morakot
874 (2009). *J.Hydrol.*, 506, 26-41, <http://dx.doi.org/10.1016/j.jhydrol.2013.02.018>, 2013.

875 Wang, C.-C.*, Lin, B.-X., Chen, C.-T., and Lo, S.-H.: Quantifying the effects of long-term
876 climate change on tropical cyclone rainfall using cloud-resolving models:
877 Examples of two landfall typhoons in Taiwan. *J. Climate*, 2015.

878 Wang, C.-C.: On the calculation and correction of equitable threat score for model
879 quantitative precipitation forecasts for small verification areas: The example of
880 Taiwan. *Wea. Forecasting*, 29, 788–798, doi:10.1175/WAF-D-13-00087.1, 2014.

881 Wang, C.-C., Huang, S.-Y., Chen, S.-H., Chang, C.-S., and Tsuboki, K.: Cloud resolving
882 typhoon rainfall ensemble forecasts for Taiwan with large domain and
883 extended range through time-lagged approach. *Wea. Forecasting*, 31, 151–172,
884 doi:10.1175/WAF-D-15-0045.1, 2016.

885 Wang, C.-C., Li, M.-S., Chang, C.-S., Chuang, P.-Y., Chen, S.-H., and Tsuboki, K.:
886 Ensemble-based sensitivity analysis and predictability of an extreme rainfall event
887 over northern Taiwan in the Mei-yu season: The 2 June 2017 case. *Atmos. Res.*, 259,
888 105684, <https://doi.org/10.1016/j.atmosres.2021.105684>, 2021.

889 Wang, C.-C., Tsai, C.-H., Jou, B. J.-D., and David, S. J.: Time-Lagged Ensemble
890 Quantitative Precipitation Forecasts for Three Landfalling Typhoons in the Philippines
891 Using the CReSS Model, Part I: Description and Verification against Rain-Gauge
892 Observations. *Atmosphere*, 13, 1193, <https://doi.org/10.3390/atmos13081193>, 2022.

893 Wang, C.-C., and Nguyen, D. V.: Investigation of an extreme rainfall event during 8–12
894 December 2018 over central Viet Nam – Part 1: Analysis and cloud-resolving

simulation. Nat. Hazards Earth Syst. Sci., 23, 771–788, <https://doi.org/10.5194/nhess-23-771-2023>, 2023.

Wang, C.-C., Chen, S.-H., Chen, Y.-H., Kuo, H.-C., Ruppert, Jr., J. H., and Tsuboki, K.: Cloud-resolving time-lagged rainfall ensemble forecasts for typhoons in Taiwan: Examples of Saola (2012), Soulik (2013), and Soudelor (2015). Wea. Clim. Extremes, 40, 100555, <https://doi.org/10.1016/j.wace.2023.100555>, 2023.

Wilks, D. S.: Statistical Methods in the Atmospheric Sciences. Academic Press, 648 pp., ISBN 13: 978-0-12-751966-1, 10: 0-12- 751966-1, 2006.

Weyn, J.A., and Durran, D.R.: The scale dependence of initial-condition sensitivities in simulations of convective systems over the southeastern United States. Q J R Meteorol Soc., 145 (Suppl.1), 57–74, <https://doi.org/10.1002/qj.3367>, 2018.

Ying, Y., and Zhang, F.: Practical and intrinsic predictability of multi-scale weather and convectively coupled equatorial waves during the active phase of an MJO. Journal of the Atmospheric Sciences, 74(11), 3771–3785. <https://doi.org/10.1175/JAS-D-17-0157.1>, 2017.